Molecular Pharmacology Fast Forward. Published on June 13, 2008 as doi:10.1124/mol.108.048694

MOL 48694

Ethanol modulates BK_{Ca} channels by acting as an adjuvant of calcium

Jianxi Liu*, Thirumalini Vaithianathan, Kandiah Manivannan, Abby Parrill and Alex M. Dopico†

Department of Pharmacology, The University of Tennessee Health Science Center (J.L., T.V., and A.M.D.)

874 Union Avenue, Memphis, TN 38163, USA

Department of Chemistry, The University of Memphis (A.P.)

213 Smith Chemistry Building

Memphis, TN 38152-3550

Department of Physics, Astronomy, and Materials Science, Missouri State University (K.M.)

901 S. National Avenue

Springfield, MO 65897

Molecular Pharmacology Fast Forward. Published on June 13, 2008 as DOI: 10.1124/mol.108.048694
This article has not been copyedited and formatted. The final version may differ from this version.

MOL 48694

Running title: Alcohol pinpoints calcium-driven gating to modulate BK_{Ca} current

Correspondence to: Alex Dopico

Phone: 901-448-3822; Fax: 901-448-1695

Email: **adopico@utmem.edu**

Text pages: 38

Tables: none

Figures: 9

Suppl. Figs: 7

References: 52

Words in Abstract: 218

Words in Introd.: 540

Words in Disc.: 2,036

Abbreviations: BK_{Ca}, large conductance, calcium- and voltage-gated potassium; AP, action potential; RCK, regulation of conductance for K^+; G, macroscopic conductance; z, effective valence; Q, gating charge; L_0, closed/open equilibrium constant in the absence of ligand; K_O, Ca^{2+} dissociation constants in the channel open conformation; K_C, Ca^{2+} dissociation constants in the channel closed conformation; N, number of functional channels in the membrane patch; P_o, channel open probability; $V_{1/2}$, half-maximal voltage; VD-MWC, voltage-dependent Monod-Wyman-Changeux; E_{max}, maximal effect; n_H, equivalent to Hill coefficient; γ, unitary slope conductance

Molecular Pharmacology Fast Forward. Published on June 13, 2008 as DOI: 10.1124/mol.108.048694
This article has not been copyedited and formatted. The final version may differ from this version.

Abstract

Ethanol modulation of calcium- and voltage-gated potassium (slo1) channels alters neuronal excitability, cerebrovascular tone, brain function and behavior, yet the mechanism of this modulation remains unknown. Using patch-clamp electrophysiology on recombinant BK_{Ca} channels cloned from mouse brain and expressed in *Xenopus* oocytes, we demonstrate that ethanol, even at concentrations maximally effective to modulate BK_{Ca} channel function (100 mM), fails to gate the channel in absence of activating calcium. Moreover, ethanol does not modify intrinsic, voltage- or physiological magnesium-driven gating. The alcohol works as an adjuvant of calcium by selectively facilitating calcium-driven gating. This facilitation, however, renders differential ethanol effects on channel activity: potentiation at low (<10 μM) and inhibition at high (>10 μM) calcium, this dual pattern remaining largely unmodified by co-expression of brain slo1 channels with the neuronally-abundant BK_{Ca} channel $beta_4$ subunit. Calcium recognition by either of the slo1 high-affinity sensors (calcium bowl and RCK1 D362/D367) is required for ethanol to amplify channel activation by calcium. The D362/D367 site, however, is necessary and sufficient to sustain ethanol inhibition. This inhibition also results from ethanol facilitation of calcium action; in this case, ethanol favors channel dwelling in a calcium-driven, low-activity mode. The agonist-adjuvant mechanism that we advance from the calcium-ethanol interaction on slo1 might be applicable to data of ethanol action on a wide variety of ligand-gated channels.

Molecular Pharmacology Fast Forward. Published on June 13, 2008 as DOI: 10.1124/mol.108.048694
This article has not been copyedited and formatted. The final version may differ from this version.

Large conductance, calcium- and voltage-gated potassium (BK_{Ca}) channels, encoded by the *Slo1* (*KCNMA1*) gene, are ubiquitous in the nervous system. Increases in channel activity in response to membrane depolarization and/or increase in internal calcium (Ca^{2+}_i) allow BK_{Ca} channels to play an important role in action potential (AP) repolarization, after-hyperpolarizations that follow the AP or, in particular, trains of APs, and in controlling the release of neurotransmitters and neurohormones (Weiger et al., 2002; Salkoff et al., 2006).

Given the key role of BK_{Ca} channels in controlling neuronal excitability and presynaptic secretion, it is not surprising that this channel type is functionally targeted by drugs that alter nervous system physiology and, thus, behavior. Indeed, several small amphiphiles, including local and general anesthetics and alcohols, have all been reported to modulate BK_{Ca} channel activity (Weiger et al., 2002). In particular, BK_{Ca} channel activity is increased by acute exposure to ethanol concentrations obtained in circulation after alcohol consumption, i.e., ethanol <100 mM (Brodie et al., 2007). This ethanol action has been demonstrated to (1) accelerate AP repolarization in rat nucleus accumbens neurons (Martin et al., 2004), (2) decrease neuronal excitability in rat dorsal root ganglia and, thus, is linked to alcohol-related analgesia (Gruß et al., 2001), and (3) inhibit the release of oxytocin and vasopressin from neurohypophysial nerve endings, the latter effect being linked to alcohol-induced diuresis (reviewed in Brodie et al., 2007). Finally, ethanol inhibition of cerebral artery BK_{Ca} channel activity contributes to alcohol-induced cerebrovascular constriction, a drug effect associated with moderate to heavy episodic drinking (Liu et al., 2004).

Ethanol modification of BK_{Ca} channel activity is modulated by a variety of factors, including posttranslational modification of the channel-forming (slo1) subunit (Liu et al., 2006), co-expression of channel accessory subunits (Martin et al., 2004), and the lipid environment of the slo1 protein (Brodie et al., 2007). However, it is ethanol modification of slo1 channel gating that

Molecular Pharmacology Fast Forward. Published on June 13, 2008 as DOI: 10.1124/mol.108.048694
This article has not been copyedited and formatted. The final version may differ from this version.

ultimately determines changes in BK_{Ca} activity and, thus, current (Dopico et al., 1998; Dopico, 2003; Martin et al., 2004). The central role of slo in alcohol actions in the body was underscored by demonstrating that BK_{Ca} channel activation in dopamine neurons is the major mechanism underlying ethanol-induced motor intoxication in *C. elegans*. In addition, mutations introduced to *Slo* by neuronal-specific promoters in *D. melanogaster* prevent the acquisition of tolerance induced by ethanol (reviewed in Brodie et al., 2007). In synthesis, neuronal slo channel activity is modulated by ethanol, which contributes to major behavioral effects of the drug. Remarkably, the mechanisms and structural basis that determine ethanol modulation of slo1 channel gating and, thus, activity, remain unknown.

Four basic processes define slo1 channel gating: intrinsic gating (channel constitutive activity), voltage-, $Mg^{2+}{}_i$-, and $Ca^{2+}{}_i$-driven gating (Cox and Aldrich, 2000). Moreover, gating by these biological signals is determined by distinct domains in the slo1 protein: the voltage sensor; the regulation of conductance for K^+ domain 1 (RCK1), which includes both a low-affinity Ca^{2+}/Mg^{2+} recognition site involved in gating by physiological Mg^{2+} and a high-affinity Ca^{2+}-recognition site, and the "calcium bowl" region. The latter and the RCK1 sense low $Ca^{2+}{}_i$ over $Mg^{2+}{}_i$ (Xia et al., 2002; Shi et al., 2002). Our study demonstrates that ethanol itself, at concentrations that modify slo1 currents and, thus, neuronal excitability and behavior, does not gate the slo1 channel nor modifies voltage-driven gating. Instead, ethanol requires physiological $Ca^{2+}{}_i$, but not $Mg^{2+}{}_i$, to alter channel activity. Ethanol is merely an adjuvant of activating $Ca^{2+}{}_i$, which leads to differential ethanol actions on BK_{Ca} P_o and, thus, current as a function of activating ligand. Finally, pinpoint mutagenesis results identified the channel structural domains that determine ethanol facilitation of Ca^{2+}-driven gating and the differential contribution of each domain to alcohol modulation of Ca^{2+} actions.

Molecular Pharmacology Fast Forward. Published on June 13, 2008 as DOI: 10.1124/mol.108.048694
This article has not been copyedited and formatted. The final version may differ from this version.

Materials and Methods

Mutagenesis and expression. cDNAs coding for mouse brain slo1 (*mslo;* mbr5) inserted into the pBluescript vector were cut with ClaI and NotI and reinserted into the pBscMXT vector for expression in *Xenopus* oocytes. Mslo mutants were constructed using Quickchange (Stratagene). Desired mutations and lack of unwanted mutations were confirmed by sequencing at the University of Tennessee Molecular Research Center. Mslo cDNAs were linearized with SalI and transcribed *in vitro* using T3 polymerase (Ambion). BK_{Ca} $beta_4$ cDNA inserted into the pOx vector was linearized by NotI and transcribed using T3 polymerase. BK_{Ca} $beta_4$ cDNA was a generous gift from Dr. Ligia Toro (UCLA).

Oocytes were removed and defolliculated as previously described (Dopico et al., 1998). Defolliculated oocytes were transferred to ND-96 solution (mM): 96 NaCl, 2 KCl, 1.8 $CaCl_2$, 5 HEPES (pH 7.4), containing 2 mg/ml gentamicin and 2.5 mM Na^+ pyruvate. Mslo mbr5 cRNA was injected alone (0.1-1 ng/μl) or with BK_{Ca} $beta_4$ (7.5 ng/μl) cRNA, giving molar ratios ≥6:1 (β:α). cRNA injection (23 nl/oocyte) was conducted using a modified micropipette (Drummond).

Electrophysiology recordings. Immediately before recordings, oocytes were devitellinized as described (Dopico et al., 1998). Recordings were obtained from I/O patches 48-72 h after cRNA injection. The electrode solution contained (mM) 130 K^+ gluconate, 5.22 $CaCl_2$, 2.28 $MgCl_2$, 5 EGTA, 1.6 HEDTA, 15 HEPES (pH 7.35), free $Ca^{2+} = 11 \pm 0.6$ μM. Micromolar levels of external $Ca^{2+}$are widely known to improve Gigaseal formation and stability, while not modifying BK_{Ca} channel function (McManus, 1991; Priel et al., 2007). Bath solutions had varied composition, as follows. In the experiments where the free Ca^{2+}_i was set to < 1 μM, the solution contained (mM): 130 K^+ gluconate, 1 $MgCl_2$, 5 EGTA, 15 HEPES (pH 7.35). In the experiments where the free Ca^{2+}_i was set to ≥1 μM, 1.6 mM HEDTA was added. In both cases, varying amounts of $CaCl_2$ (Dopico, 2003) were used to set the free Ca^{2+} at the desired level, keeping free

Molecular Pharmacology Fast Forward. Published on June 13, 2008 as DOI: 10.1124/mol.108.048694
This article has not been copyedited and formatted. The final version may differ from this version.

Mg^{2+} constant at 1 mM. For the experiments conducted in zero Ca^{2+}_i the bath solution contained (mM): 130 K^+ gluconate, 2.9 $MgCl_2$, 5 EGTA, 1.6 HEDTA, 15 HEPES, 10 glucose (pH 7.35). For the experiments conducted in zero Mg^{2+}_i, the bath solution contained (mM): 130 K^+ gluconate, 5 EGTA, 1.6 HEDTA, 15 HEPES, 10 glucose (pH 7.35), with 5, 5.36, 6.1, 6.42, 6.63, and 6.88 mM $CaCl_2$ to achieve 1, 3, 10, 30, 100, and 300 μM free Ca^{2+}. In making the free Mg^{2+} solution having 0.3 μM free Ca^{2+}, HEDTA was omitted and 4.1 mM $CaCl_2$ was added. For the experiments with the combined 5D5N, D362A/D367A mutant at 1 mM free Ca^{2+}_i, the bath solution contained (mM): 130 K^+ gluconate, 7.5 $CaCl_2$, 1 $MgCl_2$, 5 EGTA, 1.6 HEDTA, 15 HEPES (pH 7.35). Free Ca^{2+} and Mg^{2+} were calculated using Max Chelator (Bers et al., 1994; www.stanford.edu/~cpatton/maxc.html) and experimentally validated using Ca^{2+}-sensitive/reference electrodes (Corning 476041 and 476416) as described in detail somewhere else (Dopico, 2003).

Patch electrodes were pulled from glass capillaries (Drummond) as previously described (Dopico et al., 1998). The procedure gave tip resistances of 2-5 MΩ (for macropatch recordings; see below) or 5-10 MΩ (for conventional I/O single channel recordings) when filled with electrode solution. An Ag/AgCl electrode was used as ground electrode. After excision from the oocyte, the inner side of the membrane patch was exposed to bath solution containing the desired ethanol concentration and/or free Ca^{2+}_i flowing from a computer-controlled, pressurized system (ALA). Deionized, 100% pure ethanol (American Bioanalytical) was freshly diluted in bath solution immediately before experiments. Perfusion with urea isosmotically replacing for ethanol was used as the control perfusion. Even when applied at maximally effective concentration (100 mM), ethanol failed to modify the bath solution pH, as predicted from the very weak acid properties of the alcohol: pH=7.376±0.004, 7.375±0.003, 7.364±0.004 for bath solution, bath solution plus 100 mM urea, and bath solution plus 100 mM ethanol, respectively (n=35).

Molecular Pharmacology Fast Forward. Published on June 13, 2008 as DOI: 10.1124/mol.108.048694
This article has not been copyedited and formatted. The final version may differ from this version.

Isosmotic control solution had no effect on slo1 channel P_o (n=11). Iberiotoxin (Alomone) was applied to the extracellular side of outside-out (O/O) patches. The electrode and bath solutions used in O/O recordings respectively corresponded to the bath and electrode solutions described above with I/O recordings. Experiments were carried out at room temperature.

Both macroscopic and unitary currents were acquired using an EPC8 (HEKA) amplifier and digitized using a 1320 interface and pClamp8 or pClamp9 software (Axon). Macroscopic currents were evoked from I/O macropatches held at -80 mV by 200 ms-long, 10 mV depolarizing steps from -100 to 100 (or 160) mV. Currents were low-pass filtered at 1 kHz with an 8-pole Bessel filter (Frequency Dev.) and sampled at 5 kHz. Average current amplitude was determined 175-200 ms after the start of the depolarizing step. Unitary currents were low-pass filtered at 7-10 kHz with an 8-pole Bessel filter and sampled at 35-50 kHz.

Kinetic modeling and analysis. Macroscopic conductance (G)-V plots were fitted to a Boltzmann function of the type $G(V) = G_{max}/1+\exp[(-V+V_{1/2})/k]$. The effective valence (z) was calculated from: $1/slope = RT/zF$, where F = 96,485 C/mol, R = 8.31 J/(mole*K), and T = absolute temperature. Data were fitted to a voltage-dependent Monod-Wyman-Changeux (VD-MWC) for allosteric proteins, using the equation $G/G_{max} = 1/\{1+[(1+Ca^{2+}_i/K_C)/(1+Ca^{2+}_i/K_O)]*L_0 *\exp[(-Q*F*V)/(R*T)]\}$, where G: macroscopic conductance, and R, T, F, and V have their usual meaning. In this VD-MWC model, four parameters of channel gating are obtained: two are Ca^{2+}-independent: Q = gating charge, L_0 = closed/open equilibrium constant in the absence of ligand, and the other are Ca^{2+}-dependent: $K_C = Ca^{2+}$ dissociation constant in the closed channel conformation, and $K_O = Ca^{2+}$ dissociation constant in the open channel conformation (Cox and Aldrich, 2000). An "*ad-hoc*" routine (Boltzmann-type of fitting) written and generously provided by Dr. Daniel Cox (Tufts University School of Medicine) was run through Igor-Pro 5 (WaveMetrics), and K_O, K_C , L_0 and Q were directly derived by fitting G/G_{max} data to the equation

Molecular Pharmacology Fast Forward. Published on June 13, 2008 as DOI: 10.1124/mol.108.048694
This article has not been copyedited and formatted. The final version may differ from this version.

given above. Boltzmann fitting routines were run using the Levenberg-Marquardt algorithm to perform nonlinear least squares fittings.

Single-channel analysis was initially performed using pClamp9 (Axon). The product of the number of channels in the patch (N) and the probability that a channel is open (P_o) was used as an index of channel steady-state activity. NP_o was calculated from the area under the curve of the Gaussian fit of all-points amplitude histograms. From a Poisson distribution of histogram data resulting from the independence and identical behavior of channel gating, NPo=xi, with i=1…n, where n is the maximum number of simultaneous conducting channels during the observation period, and x is the Area Under the Curve corresponding to each opening, as explained in our first study of ethanol action on mslo channels (Dopico et al., 1996; 1998). This method of NP_o calculation allowed us to easily identify 1) BK_{Ca} channels from contaminant ion channels that could be present in the cell membrane, avoiding the use of blockers; 2) possible subconductance states through which the BK_{Ca} channel might sojourn. If present, the method would have determined the contribution of these subconductances to the total channel activity, and their possible modulation by calcium and/or ethanol. NP_o values were obtained from gap-free recording of single channel activity for 1-3 min under each condition (control bath, ethanol, washout for any given ionic gradient).

From patches where N=1, dwell-time histograms were constructed using the half-amplitude threshold criterion from data low-pass filtered at 5-10 kHz, rendering an effective dead time for event analysis that ranges from 18-28 μs. A maximum-likelihood minimization routine was used to fit exponential curves to the distribution of open and closed-times. An F table ($P < 0.01$) was used to determine the minimum number of exponential components to appropriately fit dwell-time histogram data. The number of components in the exponential fit to the open (closed) time distribution provided a minimum estimate of the number of open (closed) states in which the

Molecular Pharmacology Fast Forward. Published on June 13, 2008 as DOI: 10.1124/mol.108.048694
This article has not been copyedited and formatted. The final version may differ from this version.

channel population sojourns (Colquhoun and Hawkes, 1983). Kinetic modeling and derivation of individual rate constants were obtained using the QuB program (www.qub.buffalo.edu).

For the construction of a simple kinetic model of channel behavior, digitized data were first idealized using the segmental *k*-means algorithm, which uses hidden-Markov models to find the most likely sequence of events in the data set and estimate model parameters. A maximum likelihood interval analysis method was used to compute the likelihood of the experimental series of open and closed times for a given set of trial rate constants and to search for the rate constants maximizing the likelihood algorithms.

Both macroscopic and microscopic data are expressed as mean ± s.e.m., where n = number of patches/cells. ANOVA and Bonferroni's test were conducted using Instat 3.05 (GraphPad), and further data plotting and fitting were performed using Origin 7.0 (Originlab).

Computational modeling. The sequences of calmodulin (pdb entry 1CLL) and the two high-affinity Ca^{2+}-binding sites of slo1 were aligned to match the first Ca^{2+}-interacting acidic residue (D56 in calmodulin, D362 in the RCK1 domain, and E912 in the calcium bowl), and models of both slo1 calcium binding sites were constructed using the homology modeling feature in MOE 2006.05 (Chemical Computing Group). Calcium and ethanol positions were transferred directly from the calmodulin crystal structure. The RCK1 domain model was modified to coordinate D367 to the calcium ion by applying distance constraints during geometry optimization of residues 366-368, with other atoms in the model held fixed using the MMFF94 forcefield.

Molecular Pharmacology Fast Forward. Published on June 13, 2008 as DOI: 10.1124/mol.108.048694
This article has not been copyedited and formatted. The final version may differ from this version.

Results

Ethanol modulation of channel activity depends on Ca^{2+}_i

We first studied ethanol action on brain BK_{Ca} (mslo) channel steady-state activity (NP_o) in the presence of highly buffered, physiological levels of free Mg^{2+}_i (1 mM), and Ca^{2+}_i (1 μM), two metal ligands that gate the BK_{Ca} channel and, thus, increase its NP_o (Xia et a;., 2002; Shi et al., 2002). Acute exposure of the cytosolic side of I/O patches expressing mslo to 100 mM ethanol, a maximally effective alcohol concentration on native and recombinant (slo1) BK_{Ca} channels (Dopico et al., 1998; Brodie et al., 2007), robustly increased NP_o (Fig. 1A, middle trace) in 7 out of 7 cells; average NP_o reached 260±22% of control ($p<0.01$) (Fig. 1B) and returned to pre-ethanol values (99±18% of control; n=7) within 3-4 min after washing in an alcohol-free solution. Activating Ca^{2+}_i appeared sufficient for ethanol to increase NP_o, as ethanol action was observed in Ca^{2+}-containing, Mg^{2+}-free solutions (Fig. 1A, bottom trace). In contrast, ethanol action was lost in internal medium containing physiological levels of Mg^{2+} but no Ca^{2+} (Fig. 1A, top trace; averages given in Fig. 1B). Therefore, physiological levels of activating Ca^{2+}_i, but not physiological Mg^{2+}_i, are necessary for ethanol to increase channel activity.

To begin to determine the mechanisms underlying ligand dependence of ethanol action, we next probed ethanol on channel function across a wide voltage range, and at Ca^{2+}_i obtained in neurons under physiological or pathological conditions (Verkhratsky, 2005). Confirming an early observation (Dopico et al., 1998), ethanol potentiated BK_{Ca} currents at submicromolar levels of Ca^{2+}_i (Fig. 2A, top), with the drug effect diminishing as Ca^{2+}_i increased. Remarkably, ethanol consistently inhibited currents when Ca^{2+}_i ranged from 10 to 100 μM (Fig. 2A, bottom). Ethanol "dual" (activation vs. inhibition) effects on mslo current were also obtained when the drug was probed at 50 mM (Fig. 3); these concentrations are submaximal (~EC_{75}) to activate neuronal BK_{Ca}

Molecular Pharmacology Fast Forward. Published on June 13, 2008 as DOI: 10.1124/mol.108.048694
This article has not been copyedited and formatted. The final version may differ from this version.

channels (Dopico et al., 1998; Brodie et al., 2007) and are reached in circulation in humans following moderate to heavy episodic alcohol consumption (Thombs et al., 2003).

Ethanol caused a leftward (current potentiation) or rightward (current reduction) shift in the normalized macroscopic current conductance (G/G_{max})-voltage (V) relationship (Fig. 2B). The resulting half-maximal voltage ($V_{1/2}$)-Ca^{2+} plots show that the "crossover" from ethanol activation (decrease in $V_{1/2}$) to inhibition (increase in $V_{1/2}$) occurs at ~10 μM free Ca^{2+}_i (Fig. 2C), which is also shown in G/G_{max} *vs.* Ca^{2+}_i plots at any given voltage (Fig. 2D). As a first approximation to understand ethanol modulation of channel gating, we fitted macroscopic current data to a VD-MWC model (Cox and Aldrich, 2000). Ethanol significantly modified the two Ca^{2+}-dependent parameters of the model: the open channel-Ca^{2+} dissociation constant (K_O) and the closed channel-Ca^{2+} dissociation constant (K_C). In contrast, ethanol failed to alter the other two parameters of the model: the closed to open equilibrium constant in the absence of Ca^{2+} (L_0), which reflects constitutive gating, and the gating charge (Q) (Fig. S1), both being Ca^{2+}-independent (Cox and Aldrich, 2000). Ethanol's lack of action on the channel gating charge is evident from identical aspects of the $V_{1/2}$ vs. Ca^{2+} plots before and after factoring Q (Figs. 2E vs. 2C). The unmodified gating charge is consistent with the parallel shifts along the voltage axis in the G/G_{max}-V plots regardless of ethanol potentiated or inhibited current (Fig. 2B); at any given Ca^{2+}_i, the channel effective valence (z) obtained from these plots (Material and Methods) was not different between control and ethanol (e.g., at 1 μM Ca^{2+}_i, z=0.34±0.01 vs. 0.33±0.02; n=9, p>0.5). Therefore, whether activating or inhibiting current, ethanol does not alter the amount of effective charge that gates the channel.

The ethanol actions on macroscopic currents in 1 mM free Mg^{2+}_i described above were identical to those in Mg^{2+}-free solution (Fig. 4), buttressing the idea that physiological Mg^{2+} is not necessary for ethanol to modulate BK_{Ca} channel gating. Collectively, our data indicate that

Molecular Pharmacology Fast Forward. Published on June 13, 2008 as DOI: 10.1124/mol.108.048694
This article has not been copyedited and formatted. The final version may differ from this version.

modulation of BK_{Ca} currents by clinically relevant concentrations of ethanol is dependent on selective targeting of Ca^{2+}-driven gating.

From G/G_{max} vs. $Ca^{2+}{}_i$ plots (e.g., Fig. 2D), we determined the maximal effect (E_{max}; $G/G_{max}=1$), the *apparent* dissociation constant ($K_{D(apparent)}$, in μM), and the equivalent to the Hill coefficient (n_H) for Ca^{2+} in both the absence and presence of ethanol: E_{max}, 0.98±0.01 vs. 0.93±0.01 ($p<0.01$); $K_{D(apparent)}$, 6.32±0.17 vs. 4.95±0.18 ($p<0.0001$); n_H, 3.84±0.21 vs. 2.55±0.15 ($p<0.0001$) (n=9). Data demonstrate that the "efficacy" of the channel natural ligand, that is Ca^{2+}, is reduced in the presence of ethanol. In the absence of changes in the number of channels present in the membrane (Dopico et al., 1998), the decreased n_H and E_{max} for Ca^{2+} caused by *acute* ethanol exposure can be explained by 1) ethanol reduction in unitary current amplitude (this would be more evident as ethanol modulation of Ca^{2+}-driven gating that leads to increased P_o reaches a "ceiling effect" at high Ca^{2+}); and/or 2) ethanol favoring ligand (Ca^{2+})-driven desensitization. To address these possibilities, we next evaluated the actions of ethanol at the single-channel level.

Ethanol effects on current result from modulation of Ca^{2+}-driven kinetics

Single-channel data obtained at different $Ca^{2+}{}_i$ and constant voltage (60 mV) and free $Mg^{2+}{}_i$ (1 mM) clearly show that ethanol failed to modify unitary current (i) amplitude (Figs. 1, 5A-D). The lack of change in i was observed within a wide voltage range (-40 to +120 mV), rendering slope conductances (γ) for the ohmic section of the i/V relationship in symmetric 130 mM K^+ of 219±21 and 221±22 pS in control and ethanol, respectively (Fig. S2A). Ethanol also failed to introduce subconductances during channel openings (Fig. 5B,D). Additionally, ethanol did not alter the high selectivity of the BK_{Ca} pore for K^+ over Na^+, as determined from the lack of change in Nernst potential shift when Na^+ substituted for K^+ (Fig. S2A). This ethanol failure to modify slope conductance and Nernst shift were consistently observed under a wide variety of divalent

Molecular Pharmacology Fast Forward. Published on June 13, 2008 as DOI: 10.1124/mol.108.048694
This article has not been copyedited and formatted. The final version may differ from this version.

conditions: 0.3 μM Ca^{2+} (Fig. S2A), at which ethanol potentiates activity; 30 μM Ca^{2+} (Fig. S2B), at which ethanol reduces activity); physiological (Fig. S2A,B) or zero Mg^{2+} (Fig. S2C). The lack of ethanol action on channel K^+ permeability and selectivity over Na^+ strongly suggests that the drug does not modify the conformation of the channel protein region involved in ion conduction. Moreover, the lack of ethanol action on channel conduction, together with ethanol failure to modify channel intrinsic gating (Fig. S3), indicates that ethanol is not acting as a solvent that alters the overall conformation of the mslo channel protein.

The dual ethanol effects on macroscopic current (Fig. 2) were paralleled by dual actions on P_o: e.g., potentiation at 0.3 μM Ca^{2+}_i (Fig. 5A vs. B) and inhibition at 30 μM Ca^{2+}_i (Fig. 5C vs. D). Thus, in the absence of changes in N and γ, ethanol effects on current are caused by drug-induced modification of P_o. Dwell-time analysis (Fig. 6) and empiric kinetic modeling (Fig. 7) explain ethanol's dual actions on P_o. At low Ca^{2+}_i (0.3 μM), both open and closed time distributions could be well fit to triple exponentials, suggesting the existence of at least three open and three closed channel states. At 30 μM Ca^{2+}_i, however, the channel enters a low-activity mode of gating, which can be seen in single-channel recordings low-passed filtered at 1 kHz as interburst periods of very low P_o lasting hundreds of milliseconds (Fig. 5C,D). At the bottom of each panel, time-expanded records low-passed at 7 kHz demonstrate that this low-activity mode includes flickery openings (arrows), resulting in an additional closed time life of ~3 msec. Thus, at 30 μM Ca^{2+}_i the closed time distribution could be satisfactorily fit to four exponentials (Fig. 6). These data with mslo channels support a previous study with native BK_{Ca} channels reporting that Ca^{2+}_i>10 μM drives channel entry into a complex, low-activity mode (Rothberg et al., 1996).

At submicromolar Ca^{2+}_i levels, ethanol drastically decreased channel long-closed events (τ_{C2} and τ_{C3}). Additionally, ethanol increased the probability of occurrence of long open-events (τ_{O3}) (Fig. 6). These ethanol actions on channel time-lives are similar to those of Ca^{2+} (Rothberg et al.,

Molecular Pharmacology Fast Forward. Published on June 13, 2008 as DOI: 10.1124/mol.108.048694
This article has not been copyedited and formatted. The final version may differ from this version.

1996) and explain the resulting increase in P_o at Ca^{2+}_i<10 μM. On the other hand, ethanol reduction of P_o at 30 μM Ca^{2+}_i (Fig. 5D vs. C) is determined by a robust reduction in the average duration of long-open events (τ_{O3}) and, more significantly, a major increase in both duration and probability of occurrence of long-closed events (τ_{C3} and τ_{C4}) (Fig. 6), as the channel spends more time in the low-activity mode (see time-expanded traces in Fig. 5D vs C). Thus, ethanol facilitates channel dwelling in a low-activity mode, resembling the actions of high micromolar Ca^{2+} on channel behavior (Rothberg et al., 1996).

Empiric, simple kinetic models explain in more detail how ethanol favors channel dwelling into the low-activity mode (Fig. 7). Based on the number of exponentials used to properly fit the dwell-times distribution without over-parametization (see Methods), we started our kinetic channel modeling by considering 3 open and 3 closed states, this initial input model (control, 0.3 μM Ca^{2+}) having 12 rate constants. Optimization of data by QuB rendered the models shown in Fig. 7A,B. Notably, we could only model the channel behavior at high Ca^{2+}_i satisfactorily by introducing an additional "state" (low-activity mode; Fig. 7C vs. A). Therefore, final (optimized) models for control and ethanol in 30 μM Ca^{2+} contain 7 "states" and 14 rate constants (Fig. 7C,D) (other formalism such as the differential equations used and their corresponding matrices are given as Supplemental information, online). Comparison of these optimized models shows that ethanol mildly diminishes the C3→C2 transition within the normal gating mode and drastically shifts the equilibrium between C3 and the low-activity mode toward the latter (× ~5 times) (Fig. 7D vs. C). These drug actions effectively favored the probability of the channel dwelling in the low activity mode: from <5% to >10% in absence and presence of ethanol. This change, together with a decrease in the probability to dwell in open states of intermediate duration (O_2) results in an overall decrease in P_o (for P_o derivation from the kinetic rate constants used in the optimized models, please also see Supplemental data; online). Ethanol actions on rate constants within the

Molecular Pharmacology Fast Forward. Published on June 13, 2008 as DOI: 10.1124/mol.108.048694
This article has not been copyedited and formatted. The final version may differ from this version.

"normal" gating mode, which explain the ethanol increase in P_o at submicromolar levels of Ca^{2+}_i, are described in Fig. 7 legend. Briefly, ethanol increase in Po results from the drug increasing the probability of the channel dwelling in O2 and decreasing the probability of the channel dwelling in C3 (Supplemental information; online).

A fact that contributes to the simplicity of the models shown in Fig. 7 is that they include only variant Ca^{2+}_i in the presence or absence of ethanol. Others determinants of gating, such as constitutive activity, Mg^{2+}_i, and gating charge, have not been considered because they do not interfere with ethanol action (Figs. 2, 4 and S1). The models, while simple, appropriately describe the ethanol-Ca^{2+} interaction and its overall effect on P_o. First, at all conditions (low and high Ca^{2+}_i, absence or presence of ethanol), P_o values calculated from the model rate constants are similar to those determined experimentally from all-points amplitude histograms (cf. P_o values in caption of Fig. 7 vs. those in Fig. 5). Second, we ran our models and obtained simulated single-channel records (Fig. S3) that look practically identical to those obtained experimentally at all conditions (Fig. 5). Collectively, dwell-time histogram analysis and kinetic modeling appear to indicate that, whether the overall effect is increased P_o (at Ca^{2+}_i <10 μM) or decreased P_o (at Ca^{2+}_i >10 μM), ethanol's final effect on slo1 activity results primarily from facilitation of Ca^{2+}-driven events and kinetic transitions. Our single-channel data and analysis, together with the lack of ethanol action on constitutive activity and voltage-driven gating (Fig. 2), and the necessity of physiologically activating Ca^{2+}_i (but not Mg^{2+}_i) for ethanol effects on current, led us to conclude that the drug, at concentrations that maximally modify slo1 channel function and current (Dopico et al., 1998; Brodie et al., 2007), cannot gate the channel in the absence of Ca^{2+}_i. Ethanol (a "co-agonist") works as a selective *adjuvant* of activating Ca^{2+}_i (the agonist), which results in current potentiation or inhibition at low and high agonist concentrations, respectively.

Molecular Pharmacology Fast Forward. Published on June 13, 2008 as DOI: 10.1124/mol.108.048694
This article has not been copyedited and formatted. The final version may differ from this version.

Our results underscore a fundamental interaction among two ligands (Ca^{2+}_i and ethanol) and a simple receptor system: the BK_{Ca}-forming mslo subunit and its immediate proteolipid environment. While homotetrameric slo1 channels appear to exist in some tissues (Papassotiriou et al., 2000), most brain BK_{Ca} channels consist of the association of slo1 and accessory subunits of the $beta_4$ subtype (Brenner et al., 2000; Salkoff et al., 2006). Thus, we probed next whether the fundamental interaction among Ca^{2+}_i, ethanol and mslo subunits that is reflected by a Ca^{2+}_i–dependent dual modulation of current by the alcohol is modified by the presence of neuronally-abundant BK_{Ca} $beta_4$ subunits.

The functional expression of a BK_{Ca} $beta_4$ subunits was determined by the refractoriness of the slo1+$beta_4$ heteromeric channel to iberiotoxin block in O/O patches, in contrast to the sensitivity of homomeric slo1 channels to this peptidyl blocker (Bukiya et al., 2007; 2008) (data not shown). At 0.3 μM Ca^{2+}_i, exposure to 100 mM ethanol consistently increased mslo+$beta_4$ channel NP_o (Fig. S4 B vs. A, and E). At 30 μM Ca^{2+}_i, however, 1000 mM ethanol caused a mild but significant decrease in mslo+$beta_4$ channel NP_o (Fig. S4 D vs. C, and E). This alcohol dual action on channel NP_o occurred in absence of changes in unitary current amplitude (Figs. S4A-D). Collectively, these data clearly indicate that within physiological calcium levels (0.3-30 μM Ca^{2+}_i), the presence of functional BK_{Ca} $beta_4$ subunits does not drastically modify ethanol pattern of modulation of slo1 channel activity (but see Discussion).

Structural domains in slo that determine ethanol facilitation of Ca^{2+}-driven gating

After determining that ethanol action on BK_{Ca} currents results from alcohol specific facilitation of Ca^{2+}-driven gating of the slo channel, we set to determine which functional domains in the slo1 subunit are involved in this fundamental alcohol action. Slo1 channels sense activating Ca^{2+} through at least three recognition sites, which can be distinguished based on their differential

Molecular Pharmacology Fast Forward. Published on June 13, 2008 as DOI: 10.1124/mol.108.048694
This article has not been copyedited and formatted. The final version may differ from this version.

selectivity for divalents and Ca^{2+} affinities: 1) the calcium-bowl region includes residues E912 and D923, thought to contribute to divalent coordination, and a penta-aspartate sequence (the 5D5N mutation drastically diminishes the Ca^{2+} sensitivity of the slo1 channel (Bian et al., 2001; Bao et al., 2004; Sheng et al., 2005; Salkoff et al., 2006); 2) the high-affinity "site" in the RCK1 domain corresponds to D362 and D367, which are thought to coordinate divalents (Xia et al., 2002); and 3) the low-affinity "site" in the RCK1 domain, determined by E374 and E399 (Shi et al., 2002). The first two sites selectively discriminate Ca^{2+} over Mg^{2+}, and nonconserved mutations in these sites drastically reduce the channel activation by low μM levels of Ca^{2+}_i. In contrast, the third site responds to activation by hundreds of μM Ca^{2+} and mM Mg^{2+} (Zeng et al., 2005).

Ca^{2+} bowl 5D5N channel mutants were characterized by a significant decrease in apparent Ca^{2+}_i sensitivity, which is evident from the right-shift in the $V_{1/2}$-Ca^{2+}_i plot when compared to that of *wt* mslo (Fig. 2B). Ethanol, however, still caused channel activation and inhibition at low and high Ca^{2+}_i levels (Fig. 8A), as it did in *wt mslo*, indicating that a functional Ca^{2+} bowl is not necessary for drug action on *slo* channels. In contrast, the D362A/D367A mutation (Xia et al., 2002) abolished ethanol inhibition (n=8), yet did not modify ethanol-potentiation (Fig. 8B). This finding indicates the involvement of the RCK1 high-affinity site in the Ca^{2+}-ethanol interaction that leads to decreased P_o. Because this decrease was due to ethanol facilitating channel dwelling in a low-activity mode (Figs. 5 and 7), ethanol results with the D362A/D367A mutant led us to hypothesize that a) at Ca^{2+}_i>>10 μM, the D362A/D367A mutant fails to enter a low-activity mode; b) ethanol fails to reduce $(N)P_o$ in this mutant. Single channel data correctly prove both hypotheses (Fig. S5). Thus, the RCK1 high-affinity site is sufficient to mediate the ethanol-calcium interaction that results in decreased P_o. Because ethanol inhibition remained in both the calcium bowl and the RCK low-affinity site mutant (Fig. 8C), it appears that the RCK1 D362/D367 site is not only sufficient but also necessary for this ethanol action.

Molecular Pharmacology Fast Forward. Published on June 13, 2008 as DOI: 10.1124/mol.108.048694
This article has not been copyedited and formatted. The final version may differ from this version.

On the other hand, mutations in each of the sites that participate in sensing micromolar, physiological levels of Ca^{2+}_i failed to modify ethanol-induced potentiation, (Fig. 8A and B). However, combining the 5D5N with the D362A/D367A mutations not only suppressed ethanol-induced inhibition (as found with the D362A/D367A mutant itself), but also consistently abolished (8/8 cells) ethanol activation (Fig. 8D). These data were obtained in 1 mM free Mg^{2+}_i and 100 μM free Ca^{2+}_i, a divalent concentration that appears sufficient to gate the channel (Xia et al., 2002; Zeng et al., 2005). Even when Ca^{2+}_i was raised to 1 mM, the combined 5D5N, D362A/D367A mutant failed to be activated by ethanol (Fig. S6). Together, data from Fig. 8A-C indicate that neither a functional Ca^{2+} bowl nor a functional RCK1 high-affinity site is necessary for ethanol-induced activation, yet each domain is sufficient for supporting this drug action.

Finally, consistent with the lack of mM Mg^{2+}_i modulation of ethanol actions (Figs. 1 and 4), the mutations E374A/E399A failed to modify BK_{Ca} activation or inhibition by ethanol (Fig. 8**C**). In conclusion, as far as submicromolar-low micromolar Ca^{2+}_i, the channel-specific and natural ligand, is sensed by one of its two high-affinity sites in the slo1 protein, ethanol modulates channel gating. In absence of slo1 crystallographic data, structural insights into the Ca^{2+}_i-ethanol interactions on these slo1 high affinity sites remain largely speculative. Crystal structures of apocalmodulin and Ca^{2+}-bound calmodulin in the presence and absence of ethanol (Chattopadhyaya et al., 1992), provide a precedent for an ethanol binding site created upon Ca^{2+} binding. This model of Ca^{2+}-dependent ethanol binding may be applicable slo1 and, thus, explain the requirement of Ca^{2+}-presence for ethanol to modulate slo1 P_o, as explored in the Discussion.

Molecular Pharmacology Fast Forward. Published on June 13, 2008 as DOI: 10.1124/mol.108.048694
This article has not been copyedited and formatted. The final version may differ from this version.

Discussion

Our study demonstrates that ethanol at concentrations that are maximally effective to modify neuronal BK_{Ca} currents and, thus, excitability, brain function, and behavior (Gruß et al., 2001; Martin et al., 2004; Brodie et al., 2007) can modulate slo1 channel activity only in the presence of activating Ca^{2+}_i. Furthermore, ethanol actions depend on the concentrations of this activating ligand. As summarized in Fig. 9, at submicromolar to low levels of μM Ca^{2+}_i, the equilibria from nonconducting to conducting states due to Ca^{2+} binding to the calcium bowl or the RCK1 high-affinity site present in the slo1 subunit are shifted by ethanol, rendering increased P_o and, thus, macroscopic current. The equilibrium from the channel "normal" gating mode to a low P_o mode is favored by higher Ca^{2+}_i and involves the RCK1 high-affinity binding site. This transition is favored by ethanol, diminishing overall P_o and, thus, current. In contrast, ethanol appears not to modify gating transitions involving divalent recognition by the RCK1 low-affinity site or movement of gating charge. In addition, ethanol fails to modify the channel intrinsic gating and ion conduction properties. Therefore, ethanol is not changing channel function by altering the overall conformation of the slo1 protein or the arrangement of the slo1 subunits in a functional tetrameric channel. Instead, ethanol action is that of a facilitator of the specific natural ligand that gates the channel, that is, Ca^{2+}_i.

A distinct feature of BK_{Ca} channel gating is that both independent and synergistic activation by transmembrane voltage and Ca^{2+}_i can occur (Cox and Aldrich, 2000; Niu et al., 2004). Synergism and independence in BK_{Ca} gating are determined by the summation of forces at the channel S6 gate, resulting from the coupling of both voltage sensors (S4) and the several Ca^{2+} sensors to the gates via peptidic "springs" in the channel structure (Niu et al., 2004). In the absence of Ca^{2+}, a linear relationship between P_o and spring distance is consistent with the linker-gating ring acting as a passive spring attached to the S6 gate (Niu et al., 2004). Evidence that

Molecular Pharmacology Fast Forward. Published on June 13, 2008 as DOI: 10.1124/mol.108.048694
This article has not been copyedited and formatted. The final version may differ from this version.

ethanol: 1) does not modify voltage-driven (Fig. 2; Fig. S1) or 2) Mg^{2+}-driven (Fig. 4) gating, and 3) cannot gate the channel in the absence of Ca^{2+} (Fig. 1) all appear to indicate that ethanol fails to modify the behavior of the passive spring attached to the S6 gate. On the other hand, we show that ethanol action is unaffected by the absence of Mg^{2+}_i (Figs. 1,4) or the E374/E399 mutations (Fig. 8C), which define the Mg^{2+} recognition site (Shi et al., 2002). The lack of ethanol interactions with voltage- and Mg^{2+}-driven gating is consistent with the idea that slo1 channel gating driven by these two biological signals may be coupled (Hu et al., 2003).

Rather, it is Ca^{2+} sensing by either the calcium bowl or the RCK1 high-affinity site that allows ethanol to modulate P_o and, thus, current. Notably, both these sites (but not the E374/ E399 site) can sense and participate in gating driven by low μM Ca^{2+}, but not mM Mg^{2+}_i (Shi et al., 2002; Zeng et al., 2005). To obtain structural insights into the Ca^{2+}-dependence of ethanol action, homology modeling of the calcium bowl and RCK1 high-affinity sites was performed. The most relevant structural template for ethanol interaction with a Ca^{2+}-binding protein is calmodulin. Fig. S7A demonstrates that ethanol *per se* does not have any effect on the apocalmodulin domain folding, which is modified solely upon Ca^{2+} binding. Ethanol is positioned in a groove near the amino end of an alpha helix, and not far away from the Ca^{2+}-coordinating residues. Remarkably, ethanol is present only when Ca^{2+} is bound to the metal coordinating residues.

To determine the relevance of this template to the high-affinity Ca^{2+}-binding sites in slo1, sequences were aligned to match the first Ca^{2+}-interacting acidic residue (Materials and Methods). The slo1 calcium bowl and RCK1 high-affinity site models include ethanol located in a groove between two alpha helixes and near their amino ends, and not far away from the Ca^{2+}-coordinating residues (Fig. S7B). The ethanol location is near but not identical to that of activating Ca^{2+}. Thus, although some kinetic actions of both ligands overlap (Fig. 5-7), Ca^{2+} and ethanol should be considered heterotropic ligands of the slo1 channel. Ethanol is near a region that allows hydrogen

Molecular Pharmacology Fast Forward. Published on June 13, 2008 as DOI: 10.1124/mol.108.048694
This article has not been copyedited and formatted. The final version may differ from this version.

bonding. This pattern is common to several proteins whose activity is modulated by ethanol (Dwyer and Bradley, 2000). This location predicts that more efficient hydrogen bond donor/acceptors than ethanol will interact more efficiently than ethanol will. Notably, trichloroethanol effects on BK_{Ca} channel activity and AP in dorsal root ganglia group-A neurons are more robust than those of ethanol (Gruß et al., 2001).

Ethanol increases Ca^{2+}-binding to calmodulin (Ohashi et al., 2004). Conceivably, an equivalent ethanol location in slo1 high-affinity binding sites could also increase their affinity for the metal and, thus, facilitate Ca^{2+}-driven gating, as demonstrated by the changes in K_C/K_O (Figs. 2 and S1), P_o (Fig. 5) and kinetic analysis (Figs. 6 and 7). Application of the apocalmodulin/ calmodulin model to slo1 high-affinity site Ca^{2+}-dependent ethanol binding might also explain why ethanol *per se* cannot activate the channel (i.e., cannot substitute for activating Ca^{2+}_i), as ethanol does not have any effect on domain folding. Finally, the residue responsible for the Ca^{2+}-induced conformational change in calmodulin (E67) has a homolog in the slo1 calcium bowl (D923). The RCK1 high affinity site, however, lacks an acidic residue at the top of the C-terminal helix. Thus, the calcium-induced conformational changes reported for calmodulin are likely to be followed more closely by those in the calcium bowl than those in the RCK1 high-affinity site. On the other hand, the RCK1 high-affinity site, but not the calcium bowl, determines ethanol-induced reduction in P_o at high μM Ca^{2+} (Figs. 8A,B). Interestingly, the contribution of these two sites to the slo1 gating process is not identical; macroscopic kinetic analysis shows that the D362/D367 site, but not the calcium bowl, slows slo1 channel deactivation at 10-300 μM Ca^{2+}_i (Zeng et al., 2005). It might be possible that the RCK1 high-affinity site favors both slow deactivation and entry into a desensitized state(s) or low-affinity mode from a common kinetic state(s) (e.g., C3 in Fig. 7). From our data, it is clear that the D362A/D367A mutant fails to enter the low-activity mode and, accordingly, is not inhibited by ethanol (Fig. S5).

Molecular Pharmacology Fast Forward. Published on June 13, 2008 as DOI: 10.1124/mol.108.048694
This article has not been copyedited and formatted. The final version may differ from this version.

Among members of the TM6 K^+ channel superfamily, slo1 presents a unique, high sensitivity to ethanol (EC_{50}~25 mM; E_{max}~100 mM, Dopico et al., 1998; Liu et al., 2006). We show that this sensitivity is secondary to ethanol modulation of Ca^{2+}-driven gating determined by Ca^{2+} interactions with the calcium bowl and the RCK1 high-affinity site, two structures missing in voltage-gated K^+ channels other than slo1 (Salkoff et al., 2006). In addition, slo1 distinctively contains an extra segment (S0), rendering an exofacial N-end (Salkoff et al., 2006). CamKII-induced phosphorylation of T107 in the S0-S1 linker of bovine aorta slo1 (*bslo*) channels (which share all relevant Ca^{2+} sensing sites with *mslo* mbr5) can gradually switch ethanol responses from activation to inhibition. These data were obtained at Ca^{2+}_i <10 μM, indicating that phosphorylation of T107 in *bslo* can override ethanol amplification of Ca^{2+} activation of slo1, and suggest a functional coupling between the S0-S1 linker and the Ca^{2+}-sensing sites involved in the Ca^{2+}-ethanol interaction.

Our study identifies a functional interaction between ethanol and Ca^{2+}_i that occurs at the BK_{Ca} channel-forming slo1 subunit. The final ethanol effect on BK_{Ca} channel gating, however, should be fine-tuned by accessory proteins that control the Ca^{2+} sensitivity of the channel complex. In particular, BK_{Ca} $beta_1$ subunits drastically increase the apparent Ca^{2+} sensitivity of slo1 channels (Brenner et al., 2000; Cox and Aldrich, 2000; Nimigean and Magleby, 2000). According to our model, an increase in apparent Ca^{2+}_i sensitivity should facilitate agonist-mediated channel dwelling into the low-activity mode (which is further favored by ethanol presence; Fig. 7), diminishing ethanol potentiation. Consistently, heterologous co-expression of $beta_1$ subunits reduces ethanol potentiation of hslo channels (Feinberg-Zadeck and Treistman, 2007).

In the brain, most native BK_{Ca} channels consist of the association of slo1 and $beta_4$ subunits (Brenner et al., 2000; Weiger et al., 2002). Within physiological levels of Ca^{2+}_i found in neurons (0.3-30 μM); the presence of $beta_4$ subunits did not modify the basic fundamental interaction

Molecular Pharmacology Fast Forward. Published on June 13, 2008 as DOI: 10.1124/mol.108.048694
This article has not been copyedited and formatted. The final version may differ from this version.

between ethanol and Ca^{2+}_i. However, the degree of ethanol-induced potentiation observed at submicromolar Ca^{2+}_i was diminished by $beta_4$. In addition, the ethanol-induced inhibition observed at 30 μM Ca^{2+}_i was somewhat increased by $beta_4$ (Fig. S4C-E vs. Figs. 5C,D). This pattern is consistent with the fact that $beta_4$ produces a very modest shift in apparent Ca^{2+}-sensitivity within the low micromolar to 30 μM Ca^{2+}_i range (Wang et al., 2006), and likely explains data showing some modulation of alcohol action on hslo channels by $beta_4$ subunits (Feinberg-Zadeck and Treistman, 2007). In brief, in the presence of Ca^{2+}_i at resting levels ($Ca^{2+}_i \leq 10$ μM), our ligand-adjuvant mechanism predicts that ethanol will potentiate BK_{Ca} currents in neurons. Indeed, this is a widespread finding (Brodie et al., 2007). On the other hand, overall Ca^{2+}_i in neurons can reach several tens of micromolar during pathophysiological processes, including excitotoxicity, seizures and aging (Tymianski and Tator, 1996). At these Ca^{2+}_i levels, ethanol will inhibit BK_{Ca} channels, impairing one of the major channel populations that protect a cell from toxic Ca^{2+}_i levels (Han et al., 2007).

Differential subunit coexpression could contribute to the relative refractoriness of native BK_{Ca} channels in nucleus accumbens neuronal dendrites to ethanol activation, when compared to their counterparts in the somata. The somatic channels express both $beta_1$ and $beta_4$ subunits while the dendritic channels express primarily $beta_1$ (Martin et al., 2004). When evaluated within a Ca^{2+}_i range at which $beta_1$-subunit coupling to slo1 effectively translates into increased P_o (Nimigean and Magleby, 2000) (i.e., increased apparent Ca^{2+}_i sensitivity), the dendritic BK_{Ca} channels are, indeed, more Ca^{2+}_i sensitive than their somatic counterparts (Martin et al., 2004). Similarly, native BK_{Ca} channels in the somata vs. nerve endings of supraoptic neurons display different current phenotypes, including apparent Ca^{2+}_i sensitivity, consistent with functional expression of slo1+$beta_1$ subunits in the somata, and expression of slo1+$beta_4$ in the nerve endings. Notably,

Molecular Pharmacology Fast Forward. Published on June 13, 2008 as DOI: 10.1124/mol.108.048694
This article has not been copyedited and formatted. The final version may differ from this version.

these nerve ending BK_{Ca} channels are sensitive to clinically relevant alcohol concentrations, whereas the somata channels are not (Brodie et al., 2007).

Clinically relevant concentrations of ethanol can modify independently of cell integrity the activity of the vast majority of ligand-gated ion channels (Lima-Landman and Albuquerque, 1989; Lovinger et al., 1990; Wu and Miller, 1994; Parker et al., 1996; Valenzuela et al., 1998; Aistrup et al., 1999; Beckstead et al., 2002; Zhang et al., 2002; Trevisani et al., 2002; Moykkynen et al., 2003; Wallner et al., 2003; Davies et al., 2005). Among inwardly rectifying channels, only G protein-activated K^+ channels (Lewohl et al., 1999) are ethanol-sensitive, and among the voltage-gated TM6 K^+ channel superfamily, BK_{Ca} are highly sensitive (Dopico et al., 1998; Martin et al., 2004; Brodie et al., 2007). Thus, we speculated whether the adjuvant-ligand interpretation that we applied to our results of ethanol-Ca^{2+} interactions on BK_{Ca} could explain some functional ethanol data obtained with ligand-gated channels other than BK_{Ca}. First, our interpretation requires ethanol to modulate activity in the presence of efficacious ligand (agonist). This requirement should be overcome in constitutively active channels, as a mutation(s) substituting for agonist-binding diminishes the energy required to drive the channel from the inactivated to the activated state (Galzi et al., 1996). Indeed, while strychnine-sensitive glycine receptors are resistant to ethanol and anesthetics in absence of glycine, constitutively active glycine receptor mutants are sensitive to these molecules (Beckstead et al., 2002). Similarly, while *wt* 5-HT3 receptors are ethanol-insensitive in absence of serotonin, constitutively active 5-HT3 mutants are ethanol-sensitive (Zhang et al., 2002).

In addition, the adjuvant-ligand interpretation requires that ethanol modulation of channel activity depends on the concentration of the agonist. In channels like slo1, where the ligand-dependent shift toward a low-activity mode or desensitized state(s) occurs only at high agonist concentrations, adjuvating the agonist with ethanol must result in ethanol-induced activation and

Molecular Pharmacology Fast Forward. Published on June 13, 2008 as DOI: 10.1124/mol.108.048694
This article has not been copyedited and formatted. The final version may differ from this version.

inhibition at low and high agonist concentrations, respectively, as shown in the present study. On the other hand, in channels with minor ligand-induced desensitization, ethanol would potentiate ligand-driven activation, the potentiation being diminished as the agonist reaches maximal effect. This also was reported for the Gly receptor (Beckstead et al., 2002). In general, in ligand-gated channels that are potentiated by ethanol, the ethanol effect would diminish with agonist concentration, as found with P2X3 (Davies et al., 2005), bungarotoxin-insensitive nAch (Aistrup et al., 1999), 5-HT3 (Parker et al., 1996), and GABA-A (Wallner et al., 2003) receptors. Finally, in channels with significant desensitization processes, our interpretation leads to the prediction that ethanol will primarily reduce activity. Thus, blocking desensitization by pharmacological agents or mutations should reduce ethanol inhibition, or even turn it into ethanol potentiation. These patterns were observed with AMPA (Moykkynen et al., 2003) and NMDA channels (Lima-Landman and Albuquerque, 1989), respectively.

In brief, our interpretation of ethanol action on BK_{Ca} channels might apply to several results obtained with ethanol on a wide variety of ligand-gated channels. The fundamental requirements of the model are that 1) ethanol cannot gate the channel *per se* unless an activating ligand (or a mutation substituting for it) is present and bound to the receptor channel; 2) ethanol, acting as an adjuvant of the activating ligand (agonist), may evoke differential responses in channel activity, which depend on agonist concentration; and 3) the ethanol site is different from that of the channel agonist (heterotropic ligands). Whether nearby or far away in the protein or protein-lipid interface, the ethanol binding site, however, must be functionally coupled to the binding site(s) of a channel agonist.

Molecular Pharmacology Fast Forward. Published on June 13, 2008 as DOI: 10.1124/mol.108.048694
This article has not been copyedited and formatted. The final version may differ from this version.

Acknowledgements

We deeply thank Jonathan Jaggar and David Armbruster for critically reading the manuscript, Daniel H. Cox for advice on macroscopic data fitting, David Colquhoun, Fred Sachs, R. Adron Harris and John J. Woodward for comments, Anna N. Bukiya for discussion, and Maria T. Asuncion-Chin for technical assistance.

References

Aistrup GL, Marszalec W and Narahashi T (1999) Ethanol modulation of nicotinic acetylcholine receptor currents in cultured cortical neurons. *Mol Pharmacol* **55**:39-49.

Bao L, Kaldany C, Holmstrand EC and Cox DH (2004) Mapping the BKCa channel's "Ca^{2+} bowl": side-chains essential for Ca^{2+} sensing. *J Gen Physiol* **123**:475-489.

Beckstead MJ, Phelan R, Trudell JR, Bianchini MJ and Mihic SJ (2002) Anesthetic and ethanol effects on spontaneously opening glycine receptor channels. *Neurochem* **82**:1343-1351.

Bers DM, Patton CW, Nuccitelli R (1994) A practical guide to the preparation of Ca2+ buffers. *Methods Cell Biol* **40:**3-29.

Bian S, Favre I and Moczydlowski E (2001) Ca^{2+}-binding activity of a COOH-terminal fragment of the Drosophila BK channel involved in Ca^{2+}-dependent activation. *Proc Natl Acad Sci USA* **98**:4776-4781.

Brenner R, Jegla TJ, Wickenden A, Liu Y and Aldrich RW (2000) Cloning and functional characterization of novel large conductance calcium-activated potassium channel beta subunits, hKCNMB3 and hKCNMB4. *J Biol Chem* **275**:6453-6461.

Brodie MS, Scholz A, Weiger TM, Dopico AM (2007) Ethanol interactions with calcium-dependent potassium channels. *Alcohol Clin Exp Res* **10**:1625-1632.

Bukiya AN, Liu J, Toro L, Dopico AM (2007) Beta1 (KCNMB1) subunits mediate lithocholate activation of large-conductance Ca2+-activated K+ channels and dilation in small, resistance-size arteries. *Mol Pharmacol* **72:**359-369.

Bukiya AN, Vaithianathan T, Toro L, Dopico AM (2008) The second transmembrane domain of the large conductance, voltage- and calcium-gated potassium channel beta(1) subunit is a lithocholate sensor. *FEBS Lett* **582:**673-678.

Chattopadhyaya R, Meador WE, Means AR, Quiocho FA (1992) Calmodulin structure refined at 1.7 A resolution. *J Mol Biol* **228**:1177-92.

Colquhoun D and Hawkes AG (1983) The principles of the stochastic interpretation of ion-channel mechanisms, in *Single Channel Recording* (Sakmann B & Neher E, eds) pp. 135-175, Plenum Press, New York, NY.

Cox DH and Aldrich RW (2000) Role of the beta1 subunit in large-conductance Ca^{2+}-activated K^+ channel gating energetics. Mechanisms of enhanced Ca^{2+} sensitivity. *J Gen Physiol* **116**:411-432.

Davies DL, Kochegarov AA, Kuo ST, Kulkarni AA, Woodward JJ, King BF, Alkana RL (2005) Ethanol differentially affects ATP-gated P2X(3) and P2X(4) receptor subtypes expressed in *Xenopus* oocytes. *Neuropharmacology* **49**:243-253.

Dopico AM (2003) Ethanol sensitivity of BK(Ca) channels from arterial smooth muscle does not require the presence of the beta 1-subunit. *Am J Physiol Cell Physiol* **284**:C1468-80.

Dopico AM, Anantharam V and Treistman SN (1998) Ethanol increases the activity of Ca^{++}-dependent K^+ (mslo) channels: functional interaction with cytosolic Ca^{++}. *J Pharmacol Exp Ther* **284**:258-268.

Dopico AM, Lemos JR, Treistman SN (1996) Ethanol increases the activity of large conductance, Ca^{2+}-activated K^+ channels in isolated neurohypophysial terminals. *Mol Pharmacol* **49:**40-48.

Dwyer DS and Bradley RJ (2000) Chemical properties of alcohols and their protein binding sites. *Cell Mol Life Sci* **57**:265-275.

Feinberg-Zadek PL, Treistman SN (2007) Beta-subunits are important modulators of the acute response to alcohol in human BK channels. *Alcohol Clin Exp Res* **31**:737-44.

Galzi JL, Edelstein SJ and Changeux J (1996) The multiple phenotypes of allosteric receptor mutants. *Proc Natl Acad Sci USA* **93**:1853-1858.

Gruß M, Henrich M, König P, Hempelmann G, Vogel W and Scholz A (2001) Ethanol reduces excitability in a subgroup of primary sensory neurons by activation of BK_{Ca} channels. *Eur. J. Neurosci.* **14**:1246-1256.

Han X, Wang F, Yao W, Xing H, Weng D, Song X, Chen G, Xi L, Zhu T, Zhou J, Xu G, Wang S, Meng L, Iadecola C, Wang G, Ma D (2007) Heat shock proteins and p53 play a critical role in K+ channel-mediated tumor cell proliferation and apoptosis *Apoptosis* **12**:1837-46.

Hu L, Shi J, Ma Z, Krishnamoorthy G, Sieling F, Zhang G, Horrigan FT and Cui J (2003) Participation of the S4 voltage sensor in the Mg^{2+}-dependent activation of large conductance (BK) K^+ channels. *Proc Natl Acad Sci USA* **100**:10488-10493.

Lewohl JM, Wilson WR, Mayfield RD, Brozowski SJ, Morrisett RA and Harris RA (1999) G-protein-coupled inwardly rectifying potassium channels are targets of alcohol action. *Nat Neurosci* **2**:1084-1090.

Lima-Landman MT and Albuquerque EX (1989) Ethanol potentiates and blocks NMDA-activated single-channel currents in rat hippocampal pyramidal cells. *FEBS Lett* **247**:61-67.

Liu J, Asuncion-Chin M, Liu P, Dopico AM (2006) CaM kinase II phosphorylation of slo Thr107 regulates activity and ethanol responses of BK channels. *Nat Neurosci*. **9**:41-9.

Liu P, Xi Q, Ahmed A, Jaggar JH, Dopico AM (2004) Essential role for smooth muscle BK channels in alcohol-induced cerebrovascular constriction. *Proc Natl Acad Sci U S A* **101**:18217-22

Lovinger DM, White G and Weight FF (1990) NMDA receptor-mediated synaptic excitation selectively inhibited by ethanol in hippocampal slice from adult rat. *J Neurosci* **10**:1372-1379

Martin G, Puig S, Pietrzykowski A, Zadek P, Emery P and Treistman S (2004) Somatic localization of a specific large-conductance calcium-activated potassium channel subtype

controls compartmentalized ethanol sensitivity in the nucleus accumbens. *J Neurosci* **24:**6563-6572.

McManus OB (1991) Calcium-activated potassium channels: regulation by calcium. *J Bioenerg Biomembr* **23**:537-560.

Moykkynen T, Korpi ER and Lovinger DM (2003) Ethanol inhibits alpha-amino-3-hydyroxy-5-methyl-4-isoxazolepropionic acid (AMPA) receptor function in central nervous system neurons by stabilizing desensitization. *J Pharmacol Exp Ther* **306**:546-555.

Nimigean CM and Magleby KL (2000). Functional coupling of the beta1 subunit to the large conductance Ca^{2+}-activated K^+ channel in the absence of Ca^{2+}. Increased Ca^{2+} sensitivity from a Ca^{2+}-independent mechanism. *J Gen Physiol* **115:**719-736.

Niu X, Qian X, and Magleby KL (2004) Linker-gating ring complex as passive spring and Ca^{2+}-dependent machine for a voltage- and Ca^{2+}-activated potassium channel. *Neuron* **42**:45-56.

Ohashi I, Pohoreki R, Morita K and Stemmer PM (2004) Alcohols increase calmodulin affinity for Ca2+ and decrease target affinity for calmodulin. *Biochim Biophys Acta* **1691**:161-167.

Papassotiriou J, Köhler R, Prenen J, Krause H, Akbar M, Eggermont J, Paul M, Distler A, Nilius B, Hoyer J (2000) Endothelial K^+ channel lacks the Ca2+ sensitivity-regulating beta subunit. *FASEB J* **14**:885-894.

Parker RM, Bentley KR and Barnes NM (1996) Allosteric modulation of 5-HT3 receptors: focus on alcohols and anaesthetic agents. *Trends Pharmacol Sci* **17**:95-99.

Priel A, Gil Z, Moy VT, Magleby KL, Silberberg SD. (2007) Ionic requirements for membrane-glass adhesion and giga seal formation in patch-clamp recording. *Biophys J* **92**:3893-3900.

Rothberg BS, Bello RA, Song L and Magleby KL (1996) High Ca^{2+} concentrations induce a low activity mode and reveal Ca^{2+}-independent long shut intervals in BK channels from rat muscle. *J Physiol* **493**:673-689.

Salkoff L, Butler A, Ferreira G, Santi C and Wei A (2006) High-conductance potassium channels of the SLO family. *Nat Rev Neurosci* **7:**921-931.

Sheng JZ, Weljie A, Sy L, Ling S, Vogel HJ and Braun AP (2005) Homology modeling identifies C-terminal residues that contribute to the Ca^{2+} sensitivity of a BK_{Ca} channel. *Biophys J* **89**:3079-3092.

Shi J, Krishnamoorthy G, Yang Y, Hu L, Chaturvedi N, Harilal D, Qin J and Cui J (2002) Mechanism of magnesium activation of calcium-activated potassium channels. *Nature* **418:**876-880.

Thombs DL, Olds RS and Snyder BM (2003) Field assessment of BAC data to study late-night college drinking. *J Stud Alcohol* **64**:322-330.

Trevisani M, Smart D, Gunthorpe MJ, Tognetto M, Barbieri M, Campi B, Amadesi S, Gray J, Jerman JC, Brough SJ, Owen D, Smith GD, Randall AD, Harrison S, Bianchi A, Davis JB, and Geppetti P (2002) Ethanol elicits and potentiates nociceptor responses via the vanilloid receptor-1. *Nat Neurosci* **5:**546-551.

Tymianski M and Tator CH (1996) Normal and abnormal ca lcium homeostasis in neurons: a basis for the pathophysiology of traumatic and ischemic central nervous system injury. *Neurosurgery* **38**:1176-1195.

Valenzuela CF, Bhave S, Hoffman P and Harris RA (1998) Acute effects of ethanol on pharmacologically isolated kainate receptors in cerebellar granule neurons: comparison with NMDA and AMPA receptors. *J Neurochem* **71**:1777-1780.

Verkhratsky A (2005) Physiology and pathophysiology of the calcium store in the endoplasmic reticulum of neurons. *Physiol Rev* **85**:201-279

Wallner M, Hanchar HJ and Olsen RW (2003) Ethanol enhances alpha 4 beta 3 delta and alpha 6 beta3 delta gamma-aminobutyric acid type A receptors at low concentrations known to affect humans. *Proc Natl Acad Sci USA* **100:**15218-15223.

Wang B, Rothberg BS, Brenner R (2006) Mechanism of beta4 subunit modulation of BK channels. *J Gen Physiol* **127:** 449-465.

Weiger TM, Hermann A and Levitan IB (2002) Modulation of calcium-activated potassium channels. *J Comp Physiol A Neuroethol Sens Neural Behav Physiol* **188:**79-87.

Wu G and Miller KW (1994) Ethanol enhances agonist-induced fast desensitization in nicotinic acetylcholine receptors. *Biochemistry* **33:**9085-9091.

Xia XM, Zeng X and Lingle CJ (2002) Multiple regulatory sites in large-conductance calcium-activated potassium channels. *Nature* **418**:880-884.

Zeng XH, Xia XM and Lingle CJ (2005) Divalent cation sensitivity of BK channel activation supports the existence of three distinct binding sites. *J Gen Physiol* **125**:273-286.

Zhang L, Hosoi M, Fukuzawa M, Sun H, Rawlings RR and Weight FF (2002) Distinct molecular basis for differential sensitivity of the serotonin type 3A receptor to ethanol in the absence and presence of agonist. *J Biol Chem* **277**:46256-46264.

Molecular Pharmacology Fast Forward. Published on June 13, 2008 as DOI: 10.1124/mol.108.048694
This article has not been copyedited and formatted. The final version may differ from this version.

Footnotes

*Jianxi Liu is a Postdoctoral Fellow of the American Heart Association SouthEast Affiliate.

†Supported by National Institutes of Health grants AA11560 and HL77424 (to A.M.D.).

Molecular Pharmacology Fast Forward. Published on June 13, 2008 as DOI: 10.1124/mol.108.048694
This article has not been copyedited and formatted. The final version may differ from this version.

Figure Legends

Fig. 1. Calcium is necessary and sufficient for ethanol to modulate BK_{Ca} channel activity. **A,** single channel recordings from the I/O patches with the cytosolic side of the patch exposed to zero Ca^{2+}_i/1 mM Mg^{2+}_i (upper), 1 μM Ca^{2+}_i/1 mM Mg^{2+}_i (middle), or zero Ca^{2+}_i/zero Mg^{2+}_i (bottom) bath solutions in the presence (right) or absence (left) of 100 mM ethanol. Channel openings are upward deflections; arrows indicate the baseline. Averages are shown in **B**. NP_o was obtained from 60 s under each condition; V=40-60 mV.

Fig. 2. Ethanol potentiates current at submicromolar Ca^{2+}_i, while inhibiting current at higher Ca^{2+}_i levels. **A,** macropatch recordings in 0.3 or 30 μM Ca^{2+}_i before and after 100 mM show ethanol dual action as a function of Ca^{2+}_i (highlighted by bolding a selective current trace: 100 mV at 0.3 μM and 40 mV at 30 μM). In addition, ethanol inhibition can be clearly seen from drug reduction of inward currents at 30 μM Ca^{2+}. **B,** whether activating or inhibiting current, ethanol causes parallel shifts in the G/G_{max}-V plots. **C,** the overall rate of decay in $V_{1/2}$ as function of Ca^{2+}_i is reduced by ethanol. **D,** a G/G_{max}-Ca^{2+} plot highlights ethanol biphasic action, which results in reduced E_{max}, K_d, and n for Ca^{2+} (see main text); V=0 mV. **E,** $z^*V_{1/2}$-Ca^{2+} plots for the conditions shown in C. For panels **B-E**: filled, control; hollow symbols, ethanol. The symbol shapes in **B**, **D** match those in the $V_{1/2}$ plots shown in **C**, **E**, with each symbol corresponding to a Ca^{2+}_i concentration given in abscissa of plots in **C**, **E**.

Fig. 3. Ethanol at concentrations obtained in blood after moderate to heavy episodic drinking potentiates current at submicromolar Ca^{2+}_i, while inhibiting current at higher Ca^{2+}_i levels. Current traces from the same I/O macropatch obtained in 1 μM (top) or 100 μM Ca^{2+}_i (bottom) in absence (left) or presence (right) of 50 mM ethanol show that at every potential step, the alcohol increases

current at Ca^{2+}_i<10 μM while decreasing current at Ca^{2+}_i>10 μM (highlighted by bolding a selective current trace: 100 mV at 1 μM and 40 mV at 100 μM free Ca^{2+}_i). Results are identical to those obtained with higher ethanol concentrations (Fig. 2). Currents were evoked and measured as described in Materials and Methods.

Fig. 4. In absence of Mg^{2+}_i, ethanol also exerts dual actions on BK_{Ca} channel currents as a function of Ca^{2+}_i. **A,** current traces from the same I/O macropatches obtained in zero Mg^{2+}_i and 3 μM Ca^{2+}_i in the absence (top) and presence (bottom) of 100 mM ethanol. As found in the presence of Mg^{2+} (Fig. 2), ethanol increases current (250% of control) at 3 μM Ca^{2+}_i (V=130 mV) while decreasing current (70% of control) at 30 μM Ca^{2+}_i (V=50 mV). **B,** G/G_{max} vs $[Ca^{2+}]_i$ plots fit to Boltzmann functions. **C,** ethanol dual action is reflected as a reduction in the steepness of the $V_{1/2}$ vs $[Ca^{2+}]_i$ plot, as found in Mg^{2+}_i presence (Fig. 2) Currents were evoked and measured as described in Materials and Methods.

Fig. 5. Ethanol dual actions on macroscopic current result from drug dual actions on P_o. Panels show unitary current traces from the same I/O patch obtained at 0.3 and 30 μM Ca^{2+}_i, before (**A, C**) and after (**B, D**) 100 mM ethanol exposure. Without modifying unitary current amplitude (see main text), ethanol increases P_o at Ca^{2+}_i below 10 μM (**B** vs. **A**) while decreasing P_o at Ca^{2+}_i above 10 μM (**D** vs. **C**). Openings are upward deflections; horizontal arrows indicate the baseline. Ca^{2+}-favors channel dwelling into ~0.5 sec-long periods of low P_o. This "low-activity mode" (Rothberg et al., 1996) includes flickery openings (see time-expanded traces obtained from the bottom trace in **C** and **D**). Ethanol further facilitates the channel dwelling into the low-activity mode (**D** vs. **C**). Data were low-passed at 7 and digitized at 35 kHz. V was set to 60 mV.

Molecular Pharmacology Fast Forward. Published on June 13, 2008 as DOI: 10.1124/mol.108.048694
This article has not been copyedited and formatted. The final version may differ from this version.

Fig. 6. Ethanol changes channel P_o by modifying both open and closed times distribution. Open and closed time distributions in the absence (left) or presence (right) of 100 mM ethanol in 0.3 μM Ca^{2+}_i (first and third rows) and 30 μM Ca^{2+}_i (second and fourth rows). Each panel shows the duration of each particular component (τ, in ms), and the relative contribution of each particular component to the total fit (in *parentheses*). The number of events was normalized before applying a Sigworth-Sine transformation as done previously (Crowley et al., 2003), which allows a better resolution of the individual components. For a description of ethanol actions on the channel dwell times, please see main text. Dot-dash lines indicate the individual exponential components of the fit, and dotted lines indicate the composite fit.

Fig. 7. Simple, empiric kinetic models identify rate constants altered by ethanol and calcium, which explain ethanol dual actions on P_o. The figure shows the final kinetic model for each experimental condition, obtained after optimization by QuB. At high Ca^{2+}_i, channel activity could be satisfactorily modeled only by introducing an additional component corresponding to the Ca^{2+}-driven, low-activity mode (**C** vs. **A**). At low Ca^{2+}_i, ethanol prevents channel entry into long-closed states by increasing the C3→C2 transition and decreasing O3→C3. In addition, ethanol stabilizes openings within the normal-activity mode by shifting the O2↔C2 equilibrium toward O2 (**B** vs. **A**). These actions explain ethanol's increase in P_o (Fig. 3). Indeed, P_o values calculated from the model rate constants (control, 0.05; ethanol, 0.2) match those obtained from all-points amplitude histograms (control, 0.04; ethanol, 0.16). At high Ca^{2+}, ethanol mildly diminishes the C3→C2 transition and drastically shifts the C3↔low activity mode equilibrium toward the latter (×5 times) (**D** vs. **C**), favoring channel dwelling within the low-activity mode. These actions explain ethanol's decrease in P_o (Fig. 3). Indeed, P_o values calculated from the rate constants (control, 0.79; ethanol, 0.7) also match those obtained from all-points amplitude histograms (control, 0.8;

Molecular Pharmacology Fast Forward. Published on June 13, 2008 as DOI: 10.1124/mol.108.048694
This article has not been copyedited and formatted. The final version may differ from this version.

ethanol, 0,67). Data for kinetic modeling were obtained from ≥5 min of continuous recording, low-pass filtered at 10 and digitized at 50 kHz. V was set to 60 mV.

Fig. 8. The two high-affinity Ca^{2+}-recognition sites in slo1 are sufficient, yet none necessary, for ethanol to modulate channel function. $V_{1/2}$-Ca^{2+}_i plots demonstrate that mutations in the Ca^{2+}-bowl (5D5N) (*n=8*) (**A**) or the RCK1 low-affinity Ca^{2+}-recognition site (E374A/E300A) (*n*=9) (**C**) fail to eliminate ethanol dual action (evident by a drug-decrease in slope; cf. Fig. 2C). In contrast, mutations in the RCK1 high-affinity site (D362A/D367A) abolish ethanol inhibition of current (*n*=9) (evident from the similar $V_{1/2}$-Ca^{2+}_i plot slopes in control and ethanol) (**B**). In all these constructs, ethanol potentiation of current at low Ca^{2+} is observed **(A-C).** In contrast, this ethanol action is lost when the 5D5N and the D362A/D367A mutations are combined (**D**). Left, single-channel recordings in absence and presence of ethanol at 0.3, 10, and 300 μM Ca^{2+}_i; V_m=80 mV; right, average responses.

Fig. 9. Cartoon illustrating our interpretation of ethanol modulation of BK_{Ca} channel activity. A lateral view (normal to the bilayer surface) of the BK_{Ca} channel is shown as a dimmer of slo1 subunits, with their relevant domains shown only in one monomer: the "core" (conducting and voltage-sensing machinery) is shown in blue; the RCKI domain is in pink; the Ca^{2+} bowl is in yellow. At lower Ca^{2+}_i, the equilibria from nonconducting (**A**) to conducting states due to Ca^{2+}-sensing by the Ca^{2+}-bowl (**B**) or by the RCK1 high-affinity site (**C**) are shifted toward the conducting states (see relative sizes of arrow heads) by ethanol, rendering increased P_o. The RCK1 high-affinity site sensing of higher [Ca^{2+}_i] makes the channel dwell in a low-activity mode (**D**), this dwelling being favored by ethanol, diminishing overall P_o. In contrast, ethanol does not modify gating involving the RCK1 low-affinity site and determined by μM-mM divalent, whether

Molecular Pharmacology Fast Forward. Published on June 13, 2008 as DOI: 10.1124/mol.108.048694
This article has not been copyedited and formatted. The final version may differ from this version.

Ca^{2+} (**E**) or Mg^{2+} (**F**). Ethanol neither affects gating involving the voltage-sensor (moving upward from **A** to **F**). Brown arrows: outward K^+ flow; plus symbols: voltage-sensor; circular "pockets": RCK1 low-affinity Ca^{2+} site; triangular notch: high-affinity Ca^2 sites in RCK1 or "bowl"; brown circles: Mg^{2+}; red drops: Ca^{2+}.

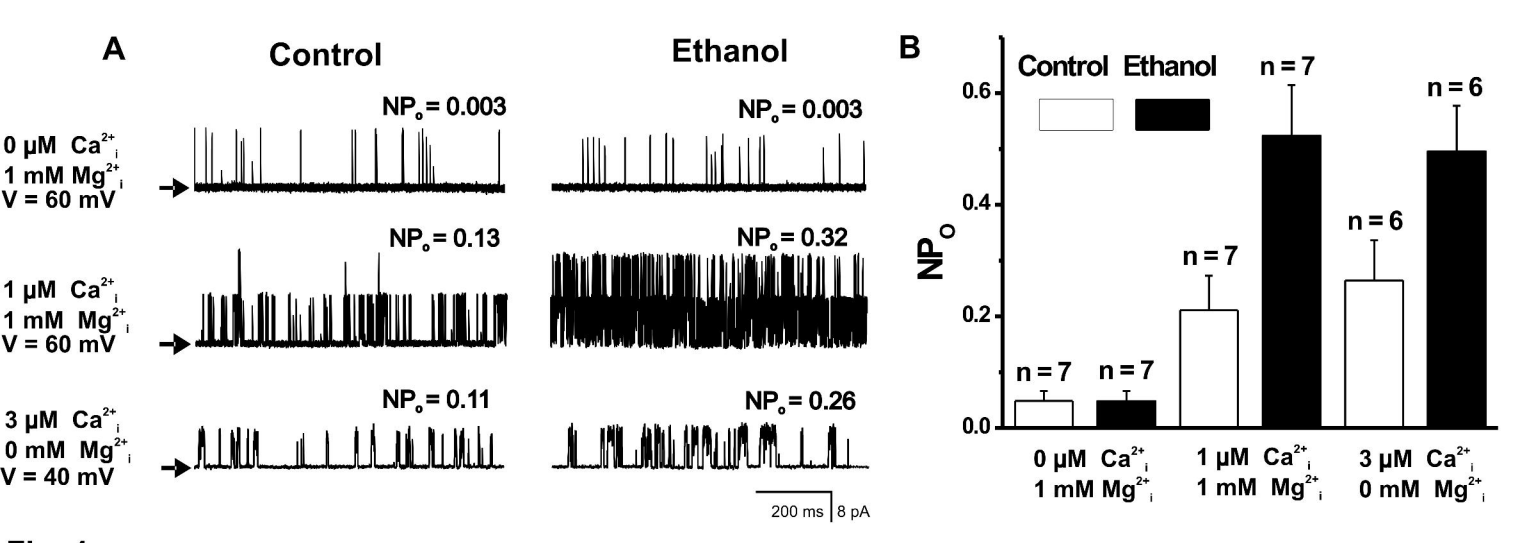
A
Control
Ethanol
NPo = 0.003
NPo = 0.003
0 μM Ca2+i
1 mM Mg2+i
V = 60 mV
NPo = 0.13
NPo = 0.32
1 μM Ca2+i
1 mM Mg2+i
V = 60 mV
NPo = 0.11
NPo = 0.26
3 μM Ca2+i
0 mM Mg2+i
V = 40 mV
200 ms
8 pA
B
Control
Ethanol
NPO
0.0
0.2
0.4
0.6
n = 7
n = 7
n = 7
n = 7
n = 6
n = 6
0 μM Ca2+i
1 mM Mg2+i
1 μM Ca2+i
1 mM Mg2+i
3 μM Ca2+i
0 mM Mg2+i

Fig. 1

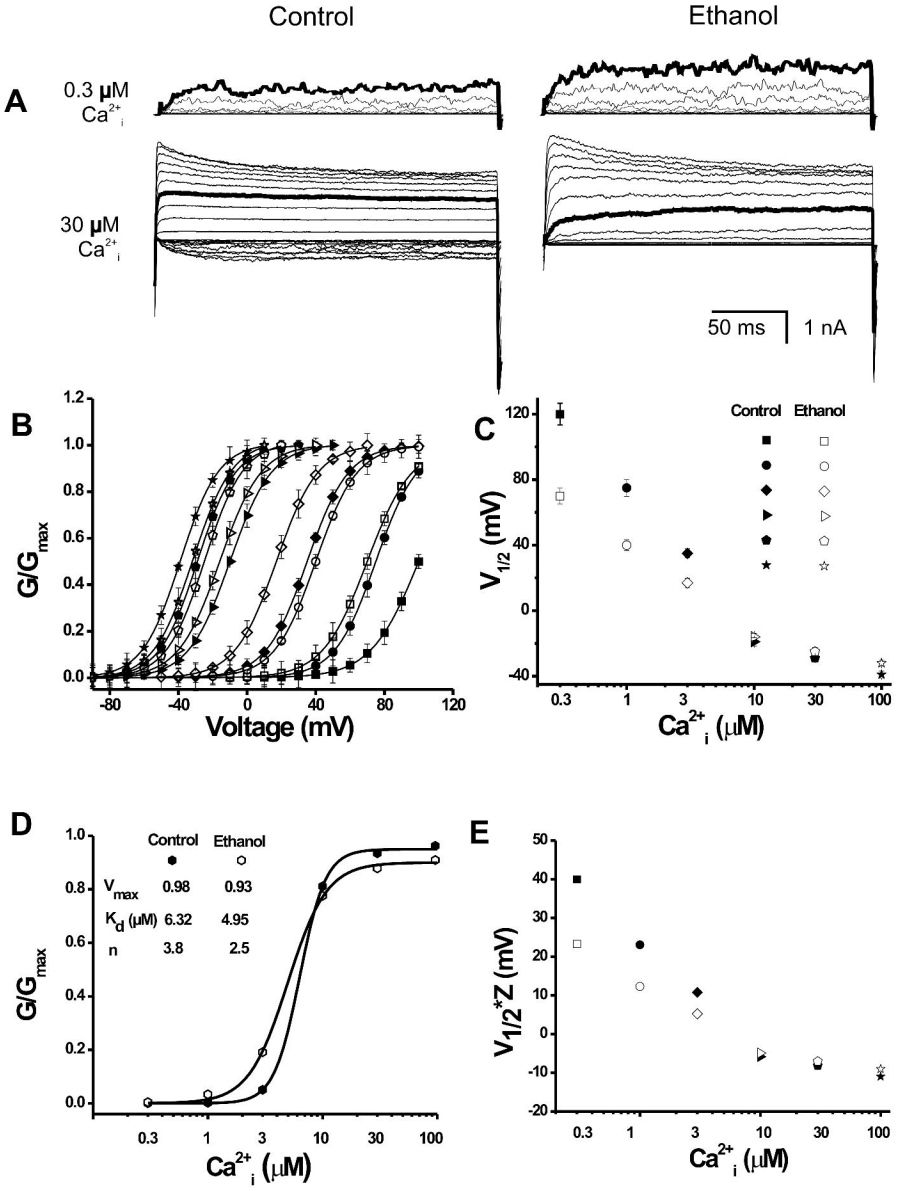
Control
Ethanol
A
0.3 μM
Ca2+i
30 μM
Ca2+i
50 ms
1 nA
B
G/Gmax
Voltage (mV)
C
Control
Ethanol
V1/2 (mV)
Ca2+i (μM)
D
Control
Ethanol
Vmax 0.98 0.93
Kd (μM) 6.32 4.95
n 3.8 2.5
G/Gmax
Ca2+i (μM)
E
V1/2*Z (mV)
Ca2+i (μM)

Fig. 2

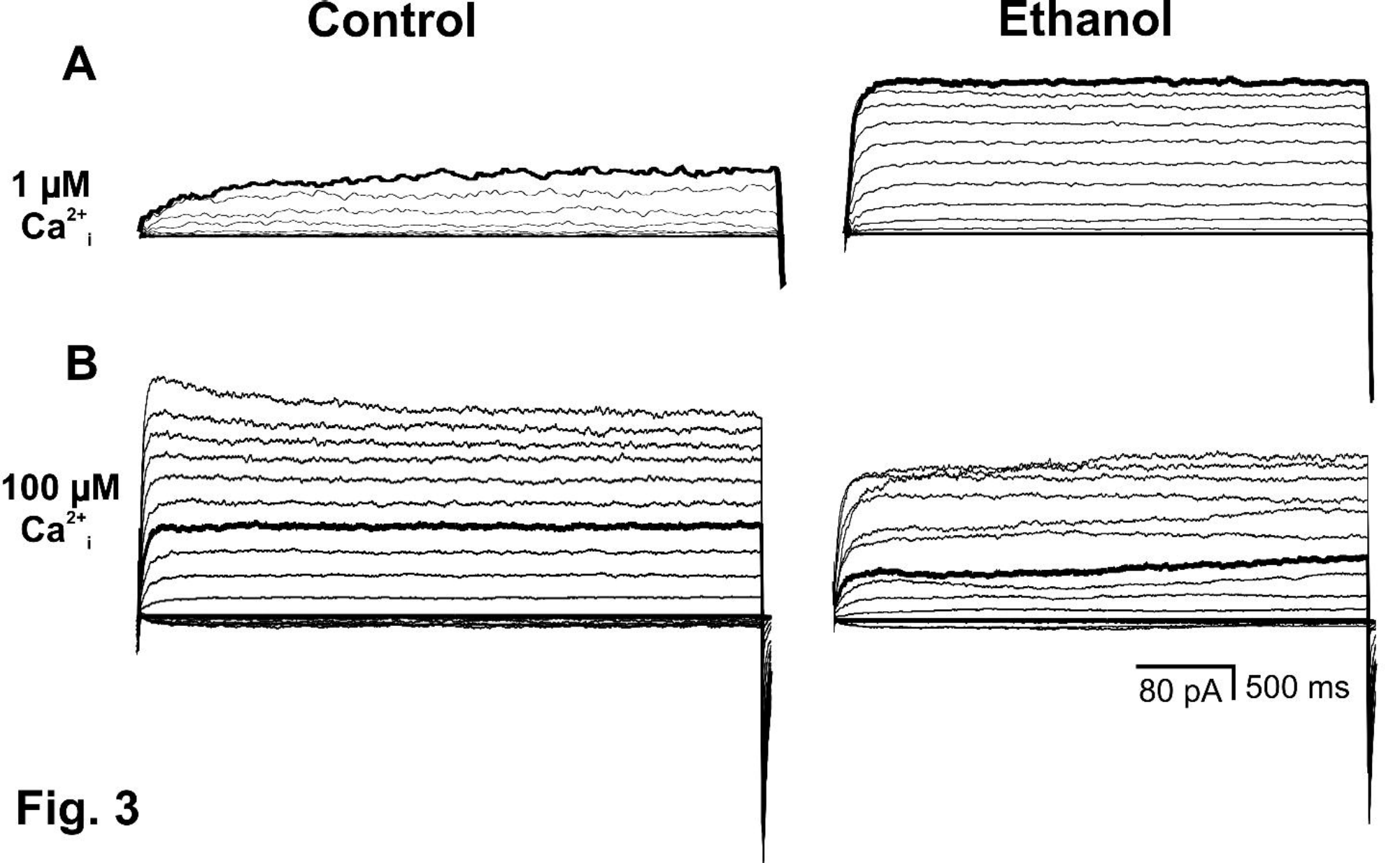

Fig. 3

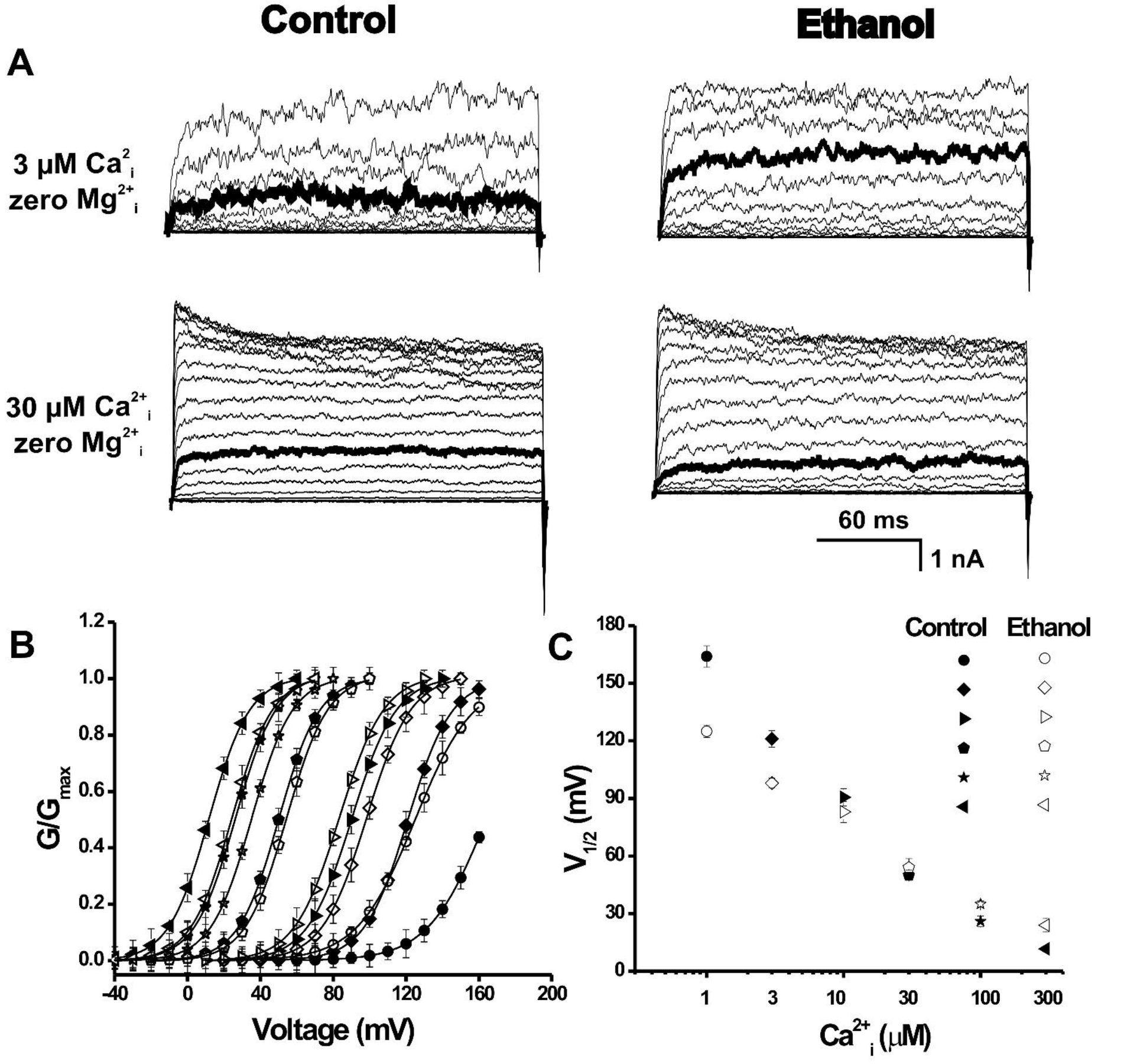
Control
Ethanol
A
3 μM Ca2 i
zero Mg2+ i
30 μM Ca2+ i
zero Mg2+ i
60 ms
1 nA
B
G/Gmax
Voltage (mV)
C
Control
Ethanol
V1/2 (mV)
Ca2+ i (μM)

Fig. 4

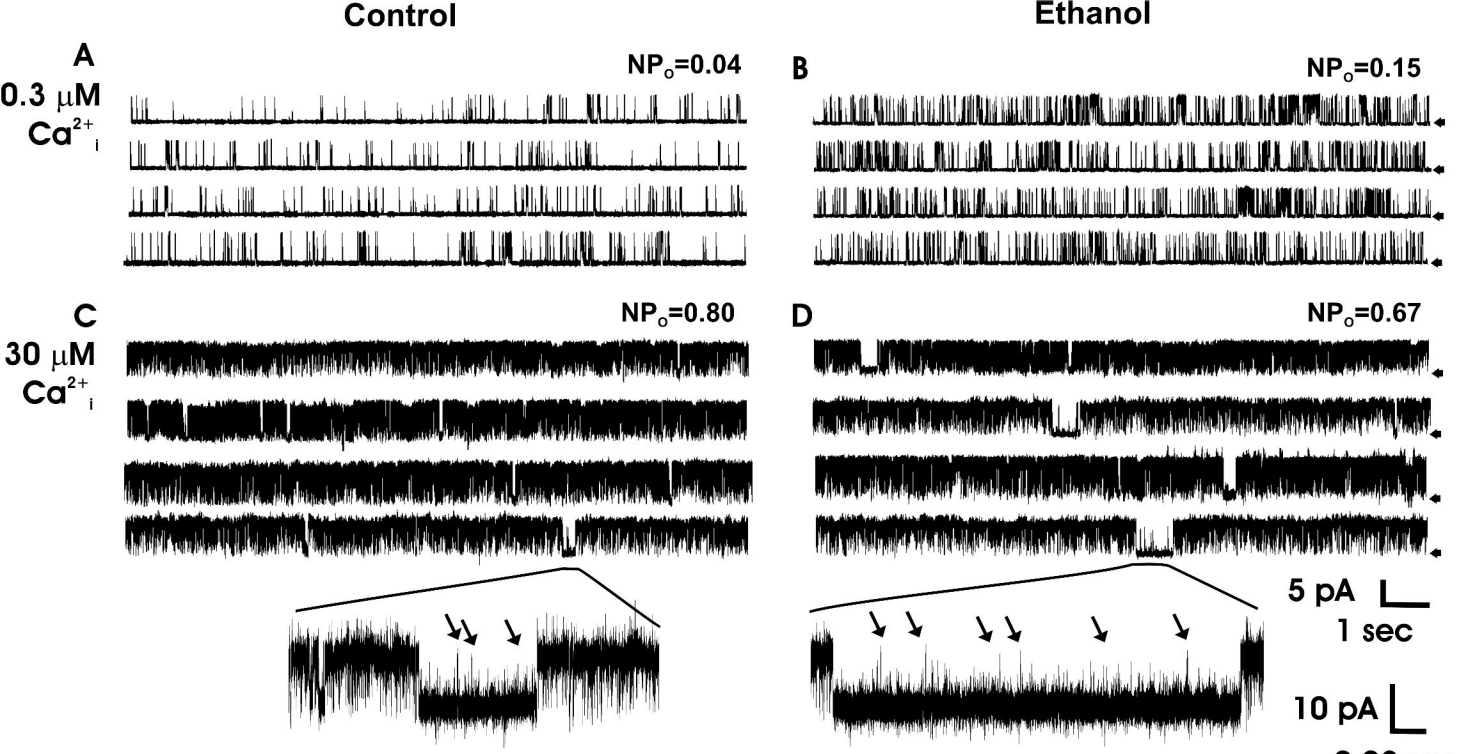
Control
Ethanol
A
0.3 μM
Ca2+i
NPo=0.04
B
NPo=0.15
C
30 μM
Ca2+i
NPo=0.80
D
NPo=0.67
5 pA
1 sec
10 pA
0.02 sec

Fig. 5

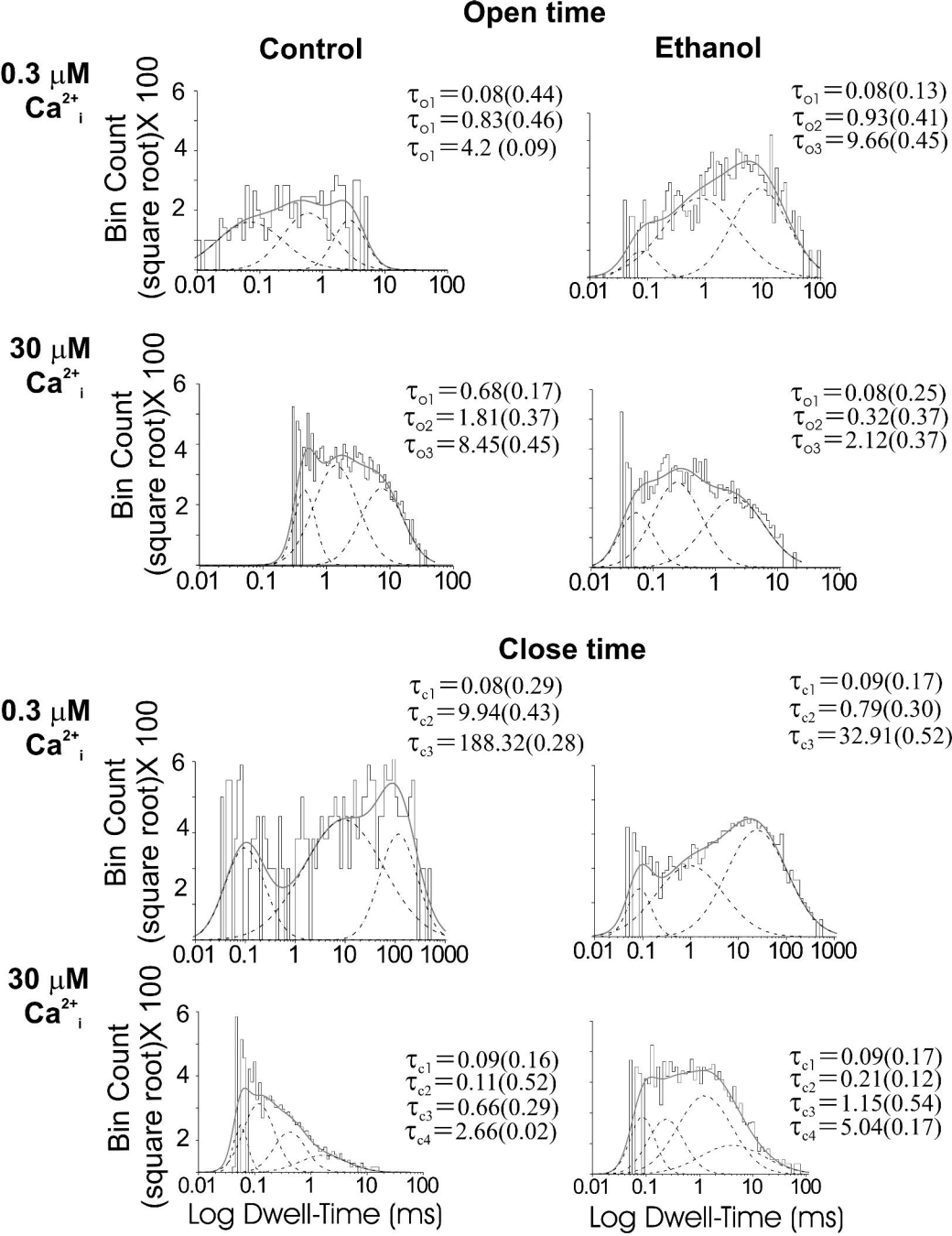
Open time
Control
Ethanol
0.3 μM Ca2+i
30 μM Ca2+i
Bin Count (square root)X 100
τo1=0.08(0.44)
τo1=0.83(0.46)
τo1=4.2 (0.09)
τo1=0.08(0.13)
τo2=0.93(0.41)
τo3=9.66(0.45)
τo1=0.68(0.17)
τo2=1.81(0.37)
τo3=8.45(0.45)
τo1=0.08(0.25)
τo2=0.32(0.37)
τo3=2.12(0.37)
Close time
τc1=0.08(0.29)
τc2=9.94(0.43)
τc3=188.32(0.28)
τc1=0.09(0.17)
τc2=0.79(0.30)
τc3=32.91(0.52)
τc1=0.09(0.16)
τc2=0.11(0.52)
τc3=0.66(0.29)
τc4=2.66(0.02)
τc1=0.09(0.17)
τc2=0.21(0.12)
τc3=1.15(0.54)
τc4=5.04(0.17)
Log Dwell-Time (ms)

Fig. 6

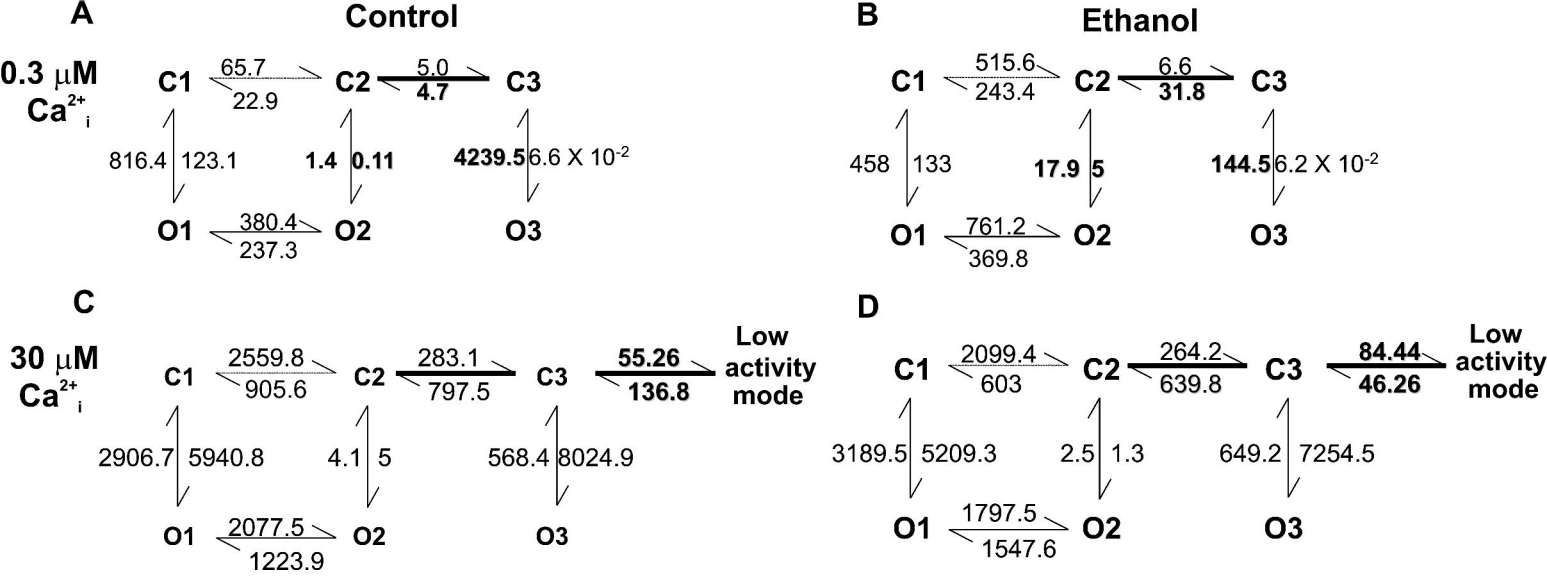
A
Control
0.3 μM
Ca2+i
C1
C2
C3
O1
O2
O3
65.7
22.9
5.0
4.7
816.4
123.1
1.4
0.11
4239.5
6.6 X 10-2
380.4
237.3
B
Ethanol
515.6
243.4
6.6
31.8
458
133
17.9
5
144.5
6.2 X 10-2
761.2
369.8
C
30 μM
Ca2+i
2559.8
905.6
283.1
797.5
55.26
136.8
Low activity mode
2906.7
5940.8
4.1
5
568.4
8024.9
2077.5
1223.9
D
2099.4
603
264.2
639.8
84.44
46.26
Low activity mode
3189.5
5209.3
2.5
1.3
649.2
7254.5
1797.5
1547.6

Fig. 7

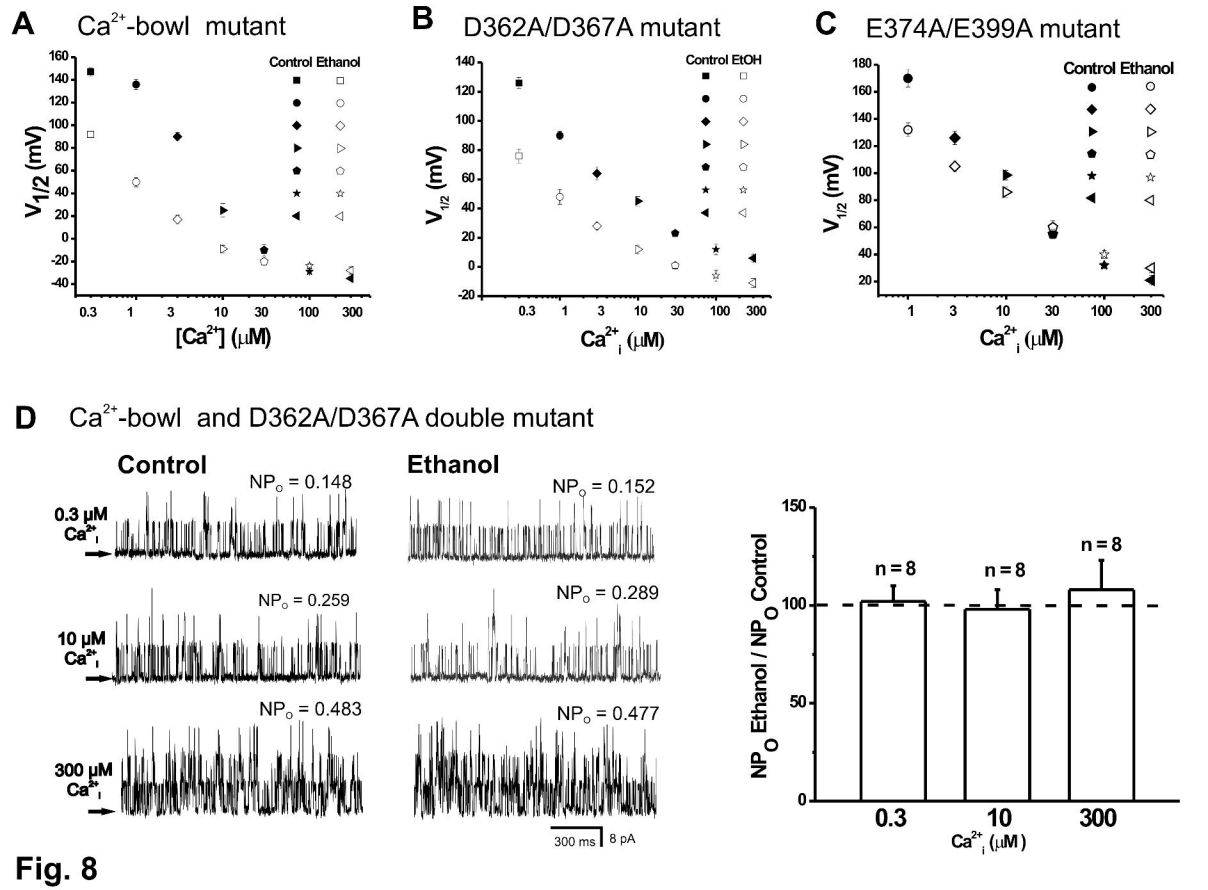
A
Ca2+-bowl mutant
Control Ethanol
V1/2 (mV)
[Ca2+] (μM)
B
D362A/D367A mutant
Control EtOH
V1/2 (mV)
Ca2+i (μM)
C
E374A/E399A mutant
Control Ethanol
V1/2 (mV)
Ca2+i (μM)
D
Ca2+-bowl and D362A/D367A double mutant
Control
Ethanol
0.3 μM Ca2+i
NPo = 0.148
NPo = 0.152
10 μM Ca2+i
NPo = 0.259
NPo = 0.289
300 μM Ca2+i
NPo = 0.483
NPo = 0.477
300 ms
8 pA
NPo Ethanol / NPo Control
n = 8
n = 8
n = 8
Ca2+i (μM)

Fig. 8

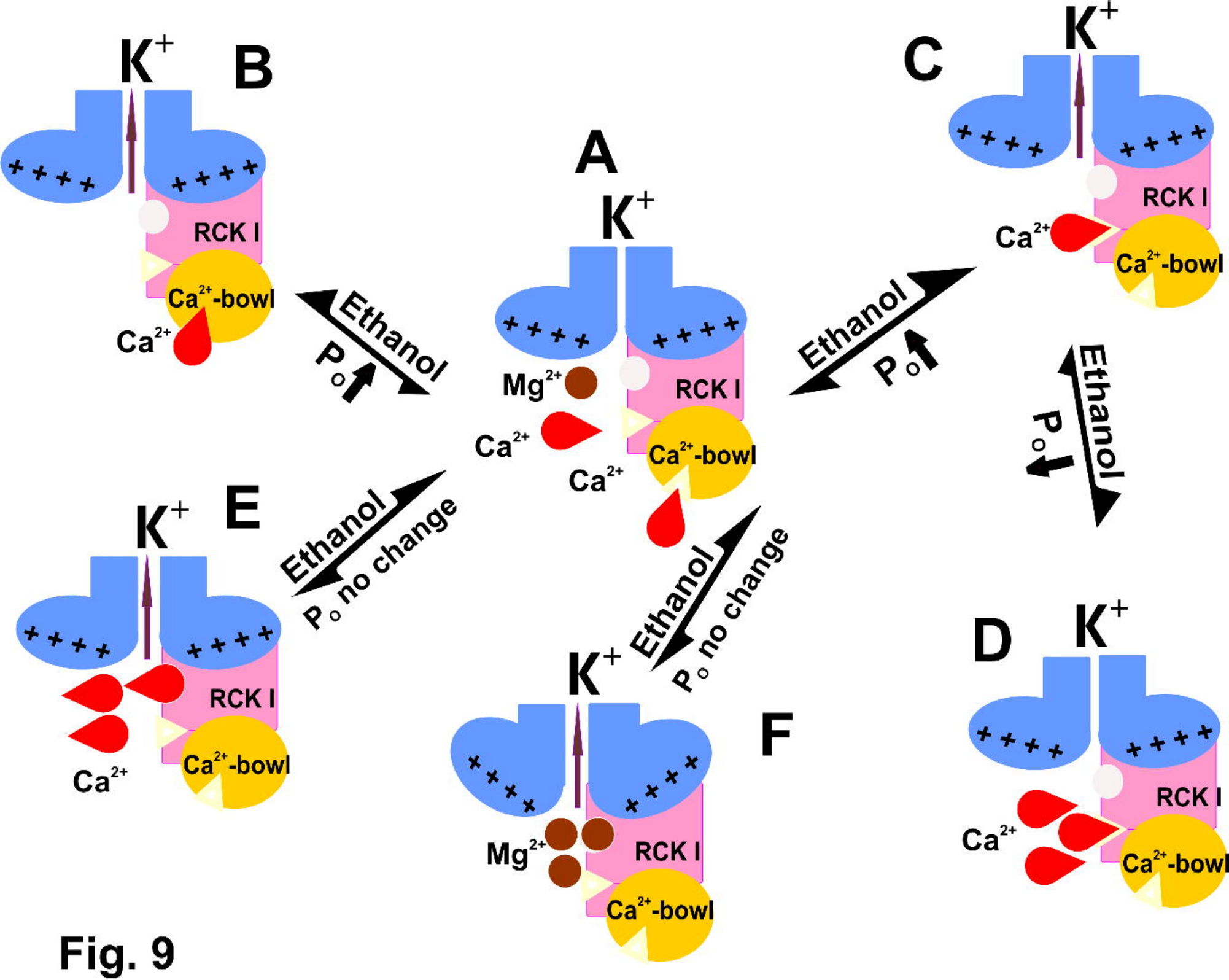
A
B
C
D
E
F
K+
RCK I
Ca2+-bowl
Ca2+
Mg2+
Ethanol
Po
Ethanol
Po no change

Fig. 9